Supplementary Information

Synthesis, spectroscopic characterization and DNA/HSA binding study of (phenyl/naphthyl)ethenyl-substituted 1,3,4-oxadiazolyl-1,2,4-oxadiazoles

João C. P. Mayer,[a] Thiago V. Acunha,[b] Oscar E. D. Rodrigues,[a] Davi F. Back,[c] Otávio Augusto Chaves,[d] Luciano Dornelles[a]* and Bernardo A. Iglesias[b]**

[a] *Departamento de Química, LabSelen-NanoBio, Universidade Federal de Santa Maria, CEP 97105-900, Santa Maria, RS, Brazil.*

[b] *Departamento de Química, Laboratório de Bioinorgânica e Materiais Porfirínicos, Universidade Federal de Santa Maria, CEP 97105-900, Santa Maria, RS, Brazil.*

[c] *Laboratório de Materiais Inorgânicos - Departamento de Química, CCNE, UFSM, Santa Maria – RS, Brazil, Zip Code 97105-900.*

[d] *Instituto SENAI de Inovação em Química Verde, Rua Morais e Silva N° 53, Bloco 09, CEP 20271030, Rio de Janeiro, RJ, Brazil.*

Table of Contents

^{1}H and ^{13}C NMR spectra of compounds 7aa-be.

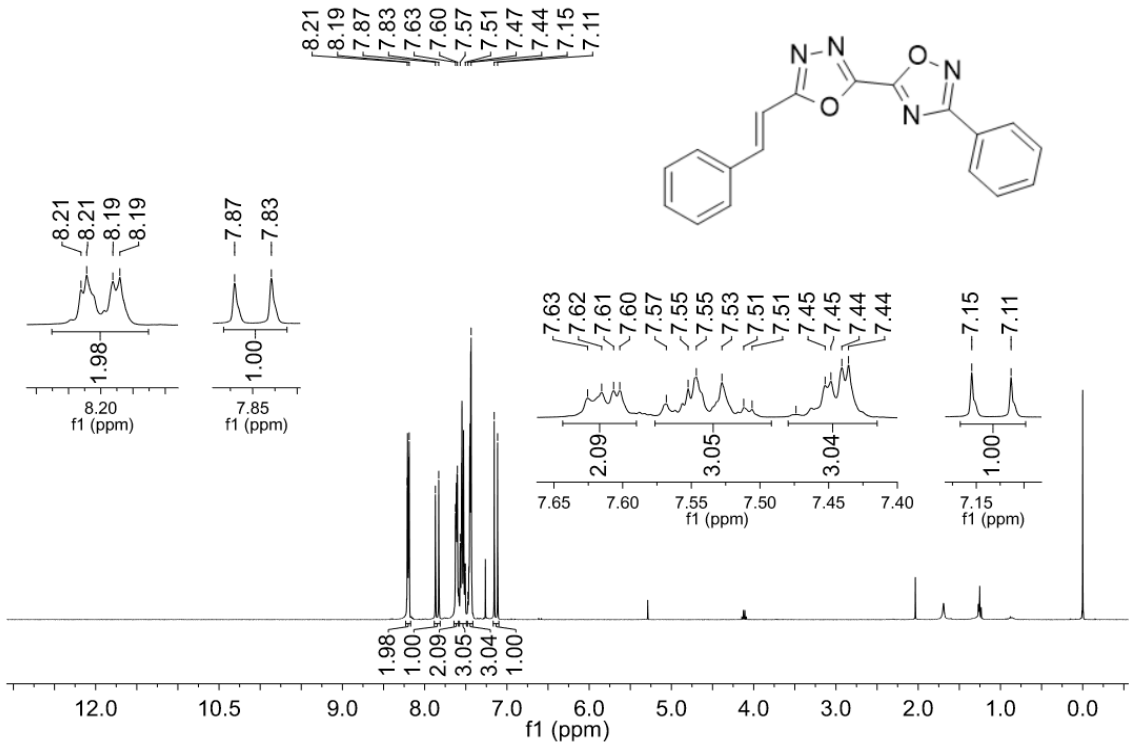

Figure S1. ^{1}H NMR spectrum ($CDCl_3$ at 400 MHz) of compound **7aa**.

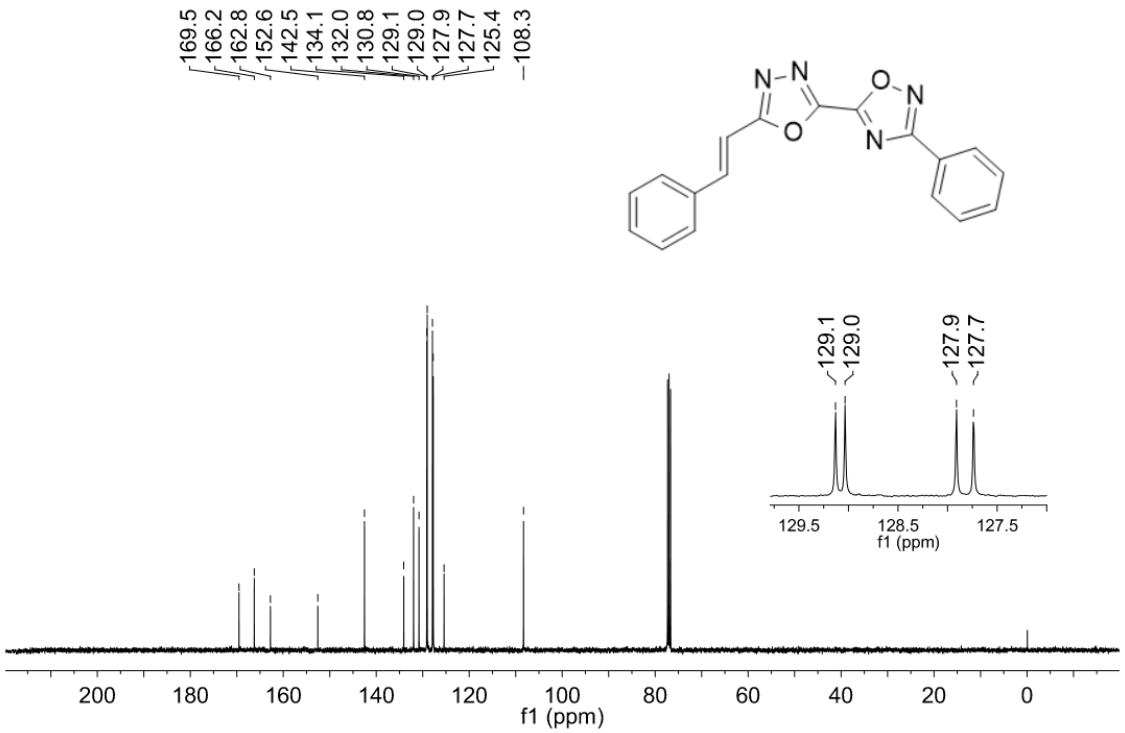

Figure S2. ^{13}C NMR spectrum ($CDCl_3$ at 100 MHz) of compound **7aa**.

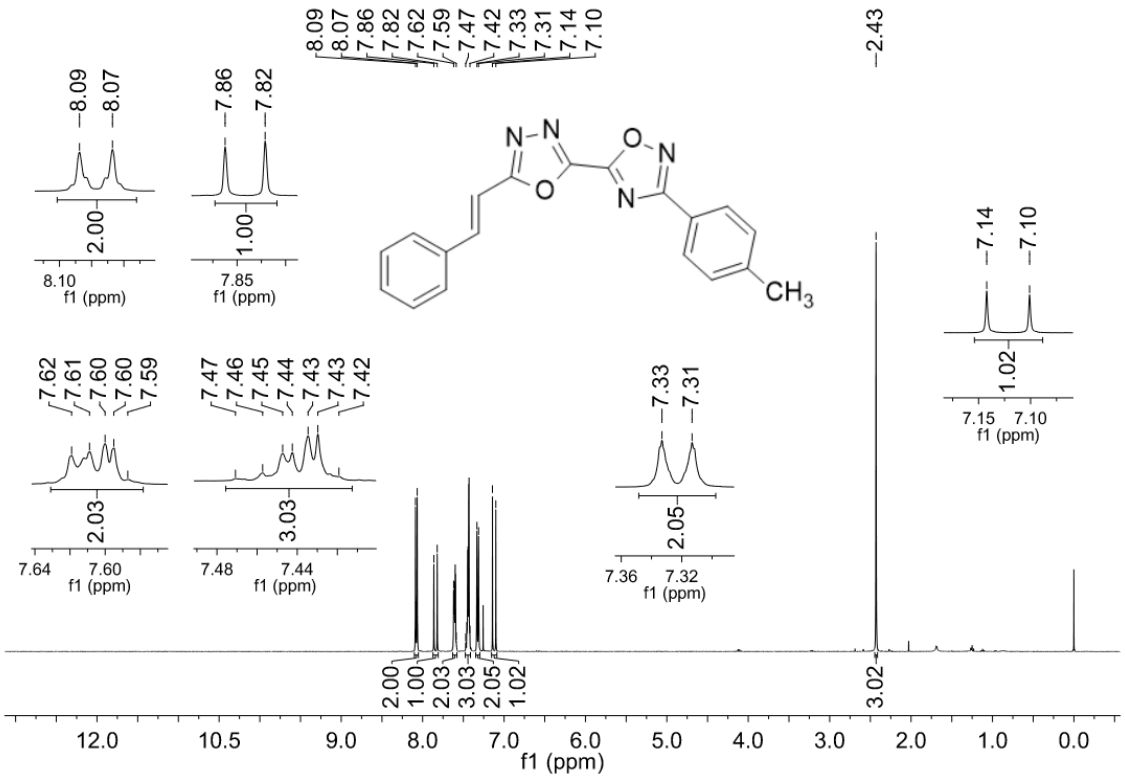

Figure S3. ^{1}H NMR spectrum ($CDCl_3$ at 400 MHz) of compound **7ab**.

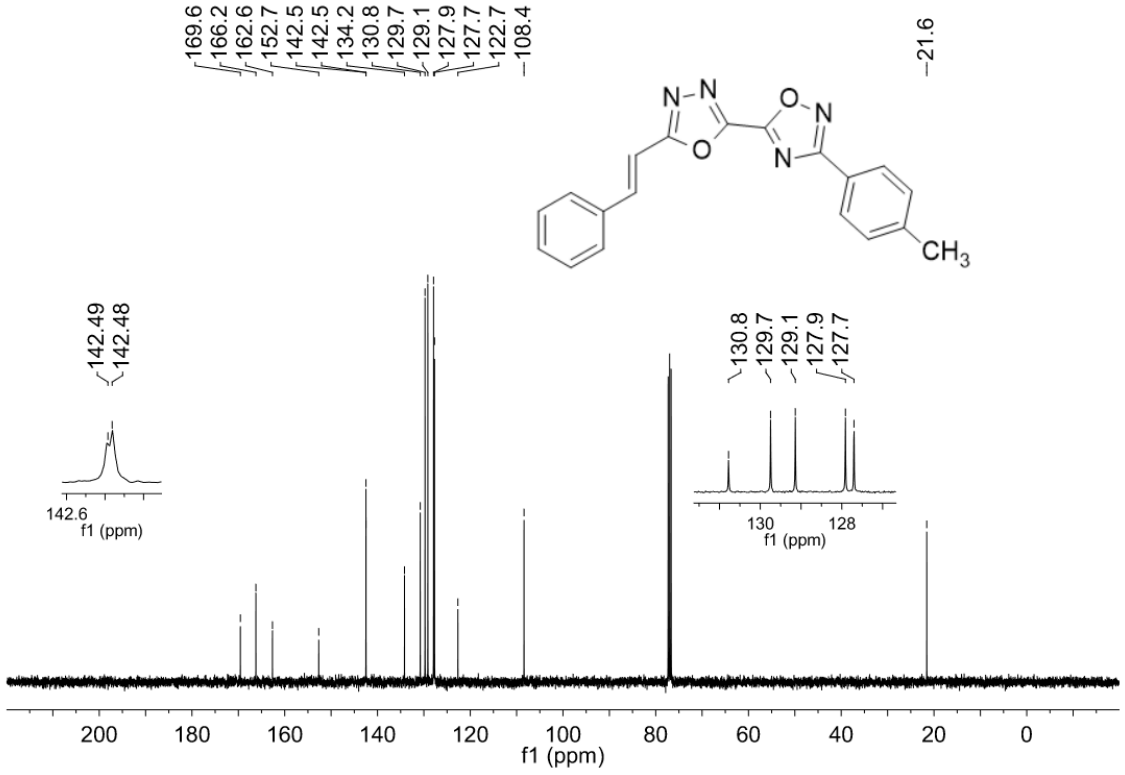

Figure S4. ^{13}C NMR spectrum ($CDCl_3$ at 100 MHz) of compound **7ab**.

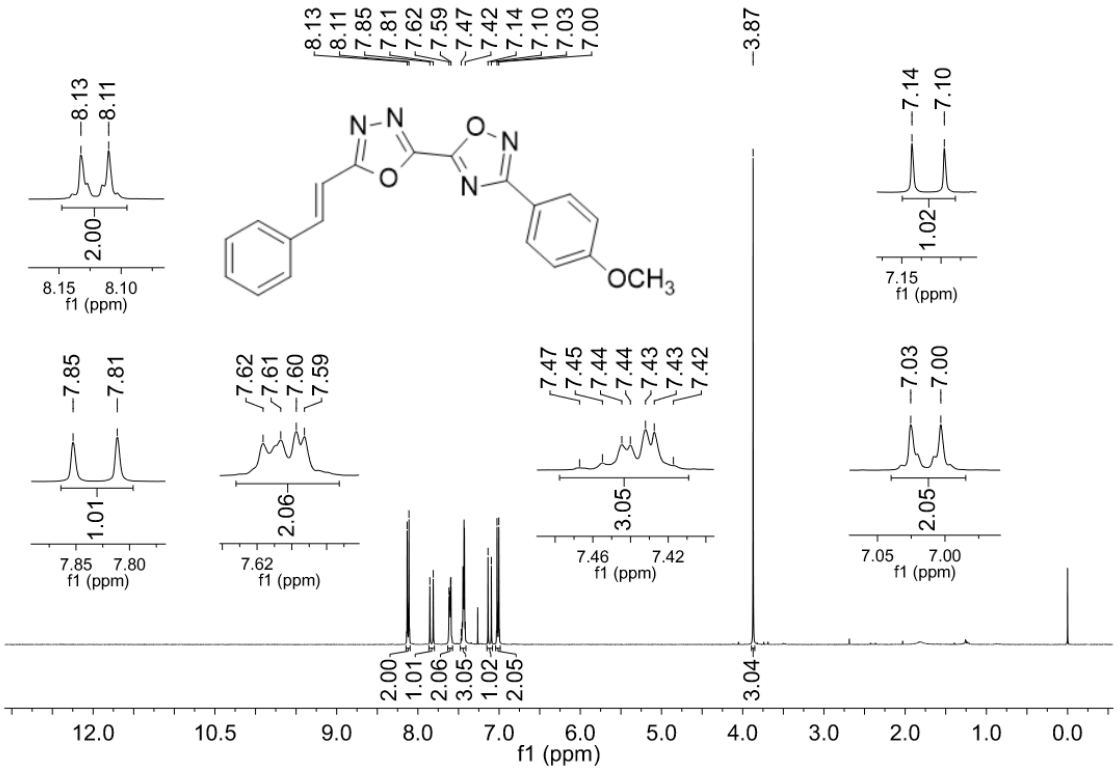

Figure S5. ^{1}H NMR spectrum ($CDCl_3$ at 400 MHz) of compound **7ac** (δ, TMS).

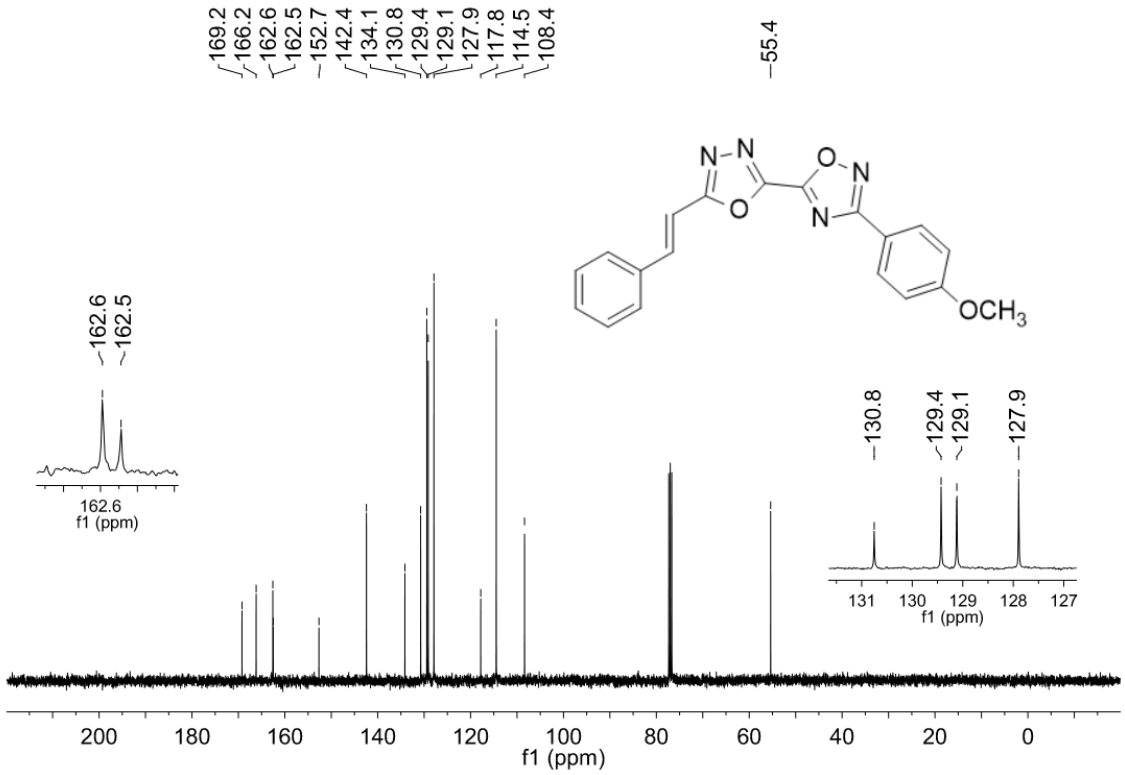

Figure S6. ^{13}C NMR spectrum ($CDCl_3$ at 100 MHz) of compound **7ac**.

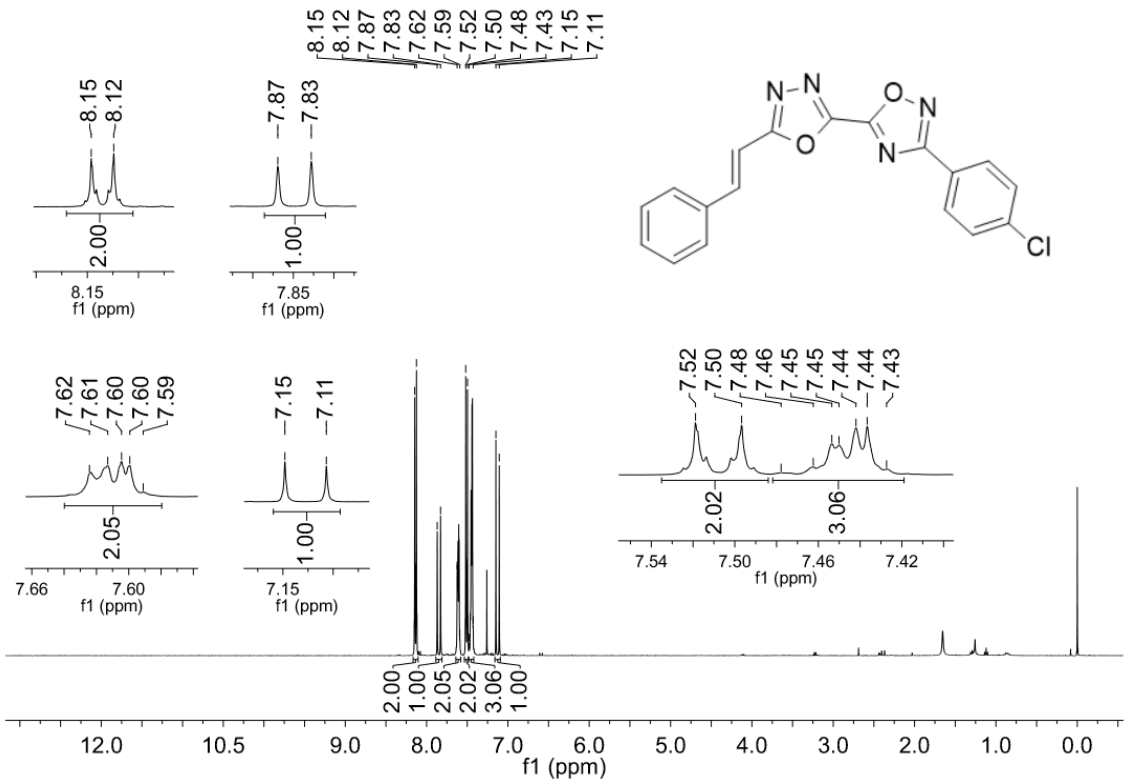

Figure S7. ^{1}H NMR spectrum ($CDCl_3$ at 400 MHz) of compound **7ad**.

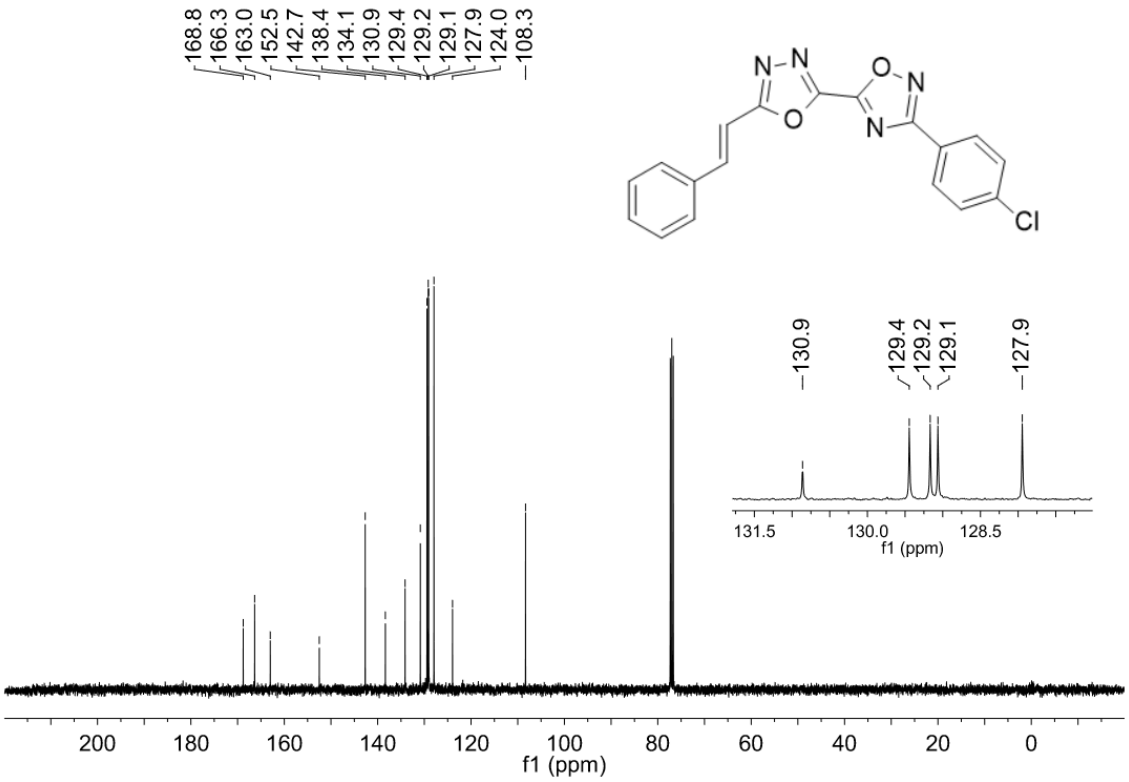

Figure S8. ^{13}C NMR spectrum ($CDCl_3$ at 100 MHz) of compound **7ad**.

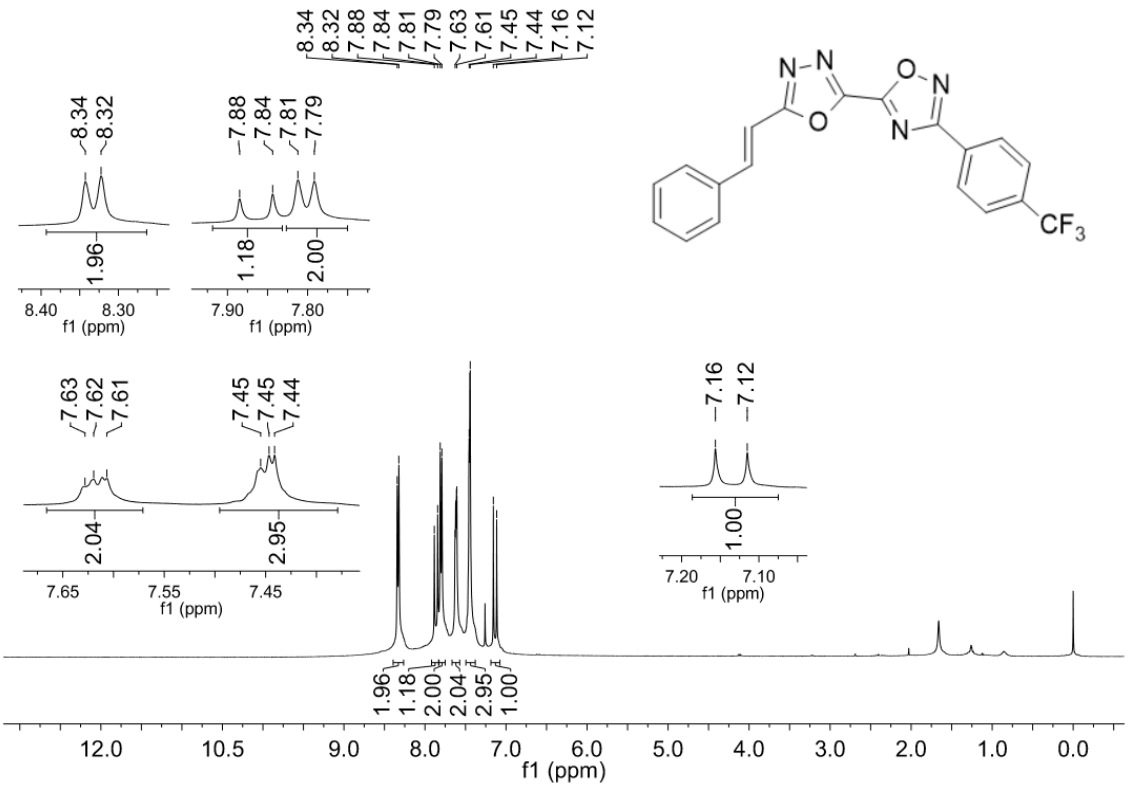

Figure S9. ^{1}H NMR spectrum ($CDCl_3$ at 400 MHz) of compound **7ae**.

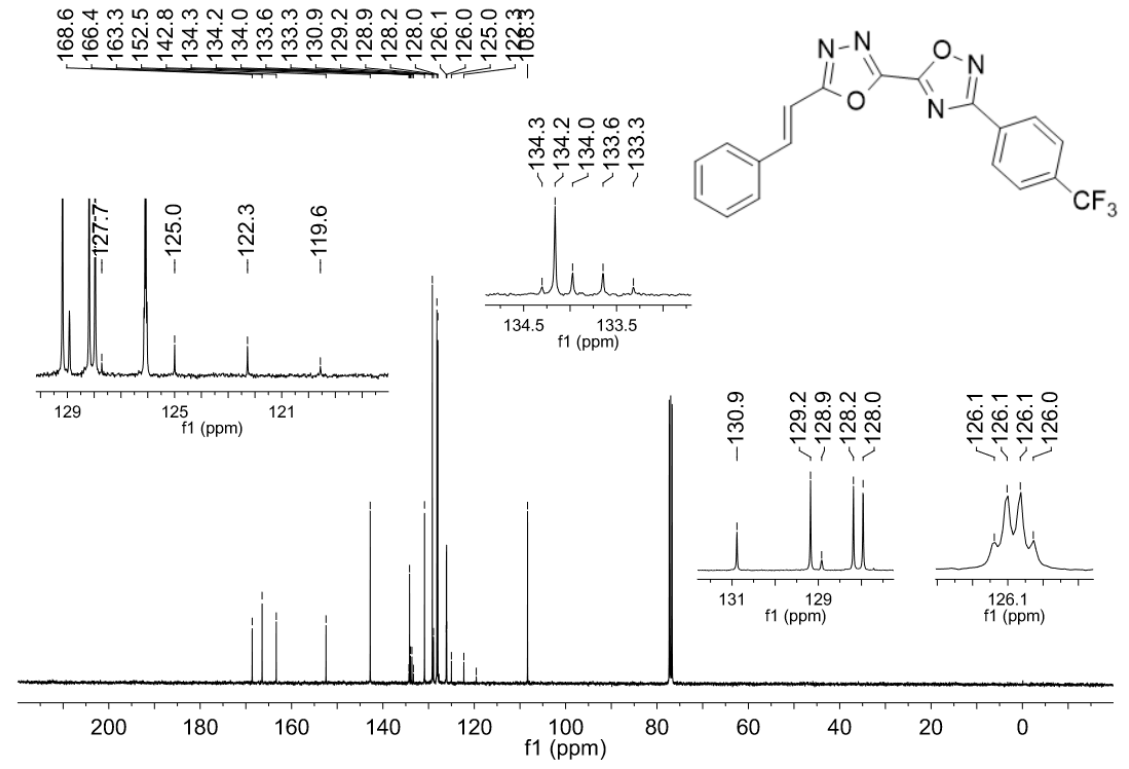

Figure S10. ^{13}C NMR spectrum ($CDCl_3$ at 100 MHz) of compound **7ae**.

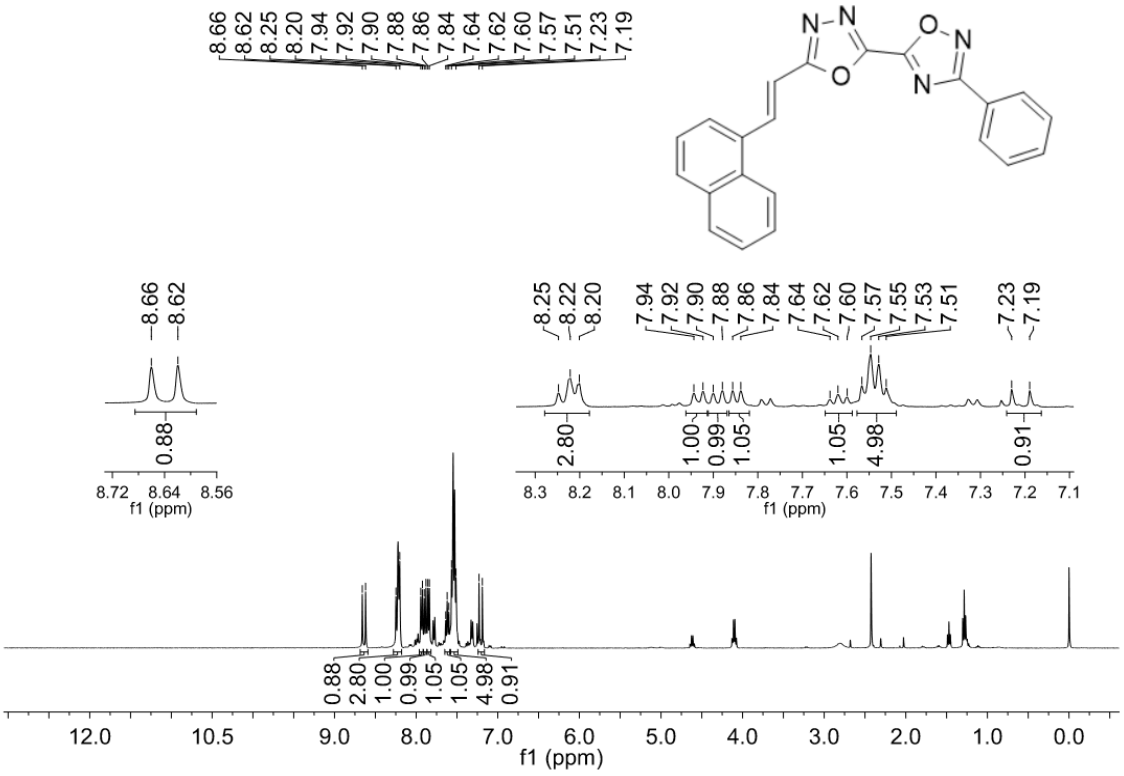

Figure S11. ^{1}H NMR spectrum ($CDCl_3$ at 400 MHz) of compound **7ba**.

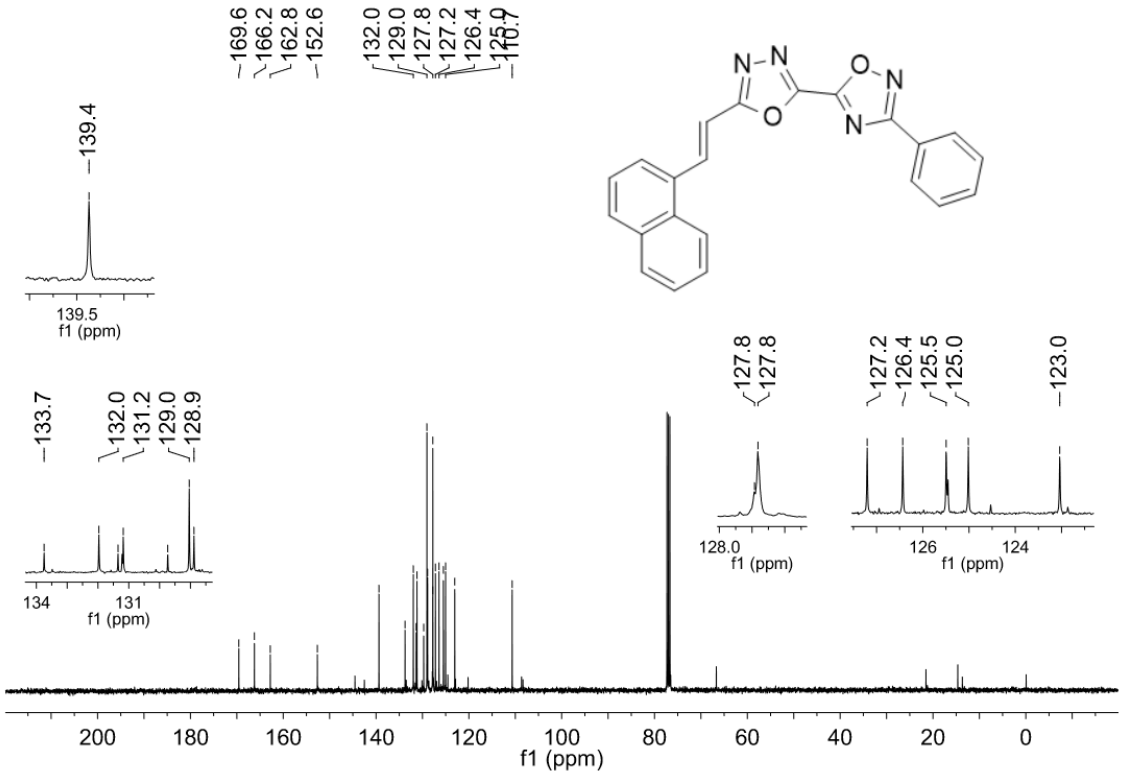

Figure S12. ^{13}C NMR spectrum ($CDCl_3$ at 100 MHz) of compound **7ba**.

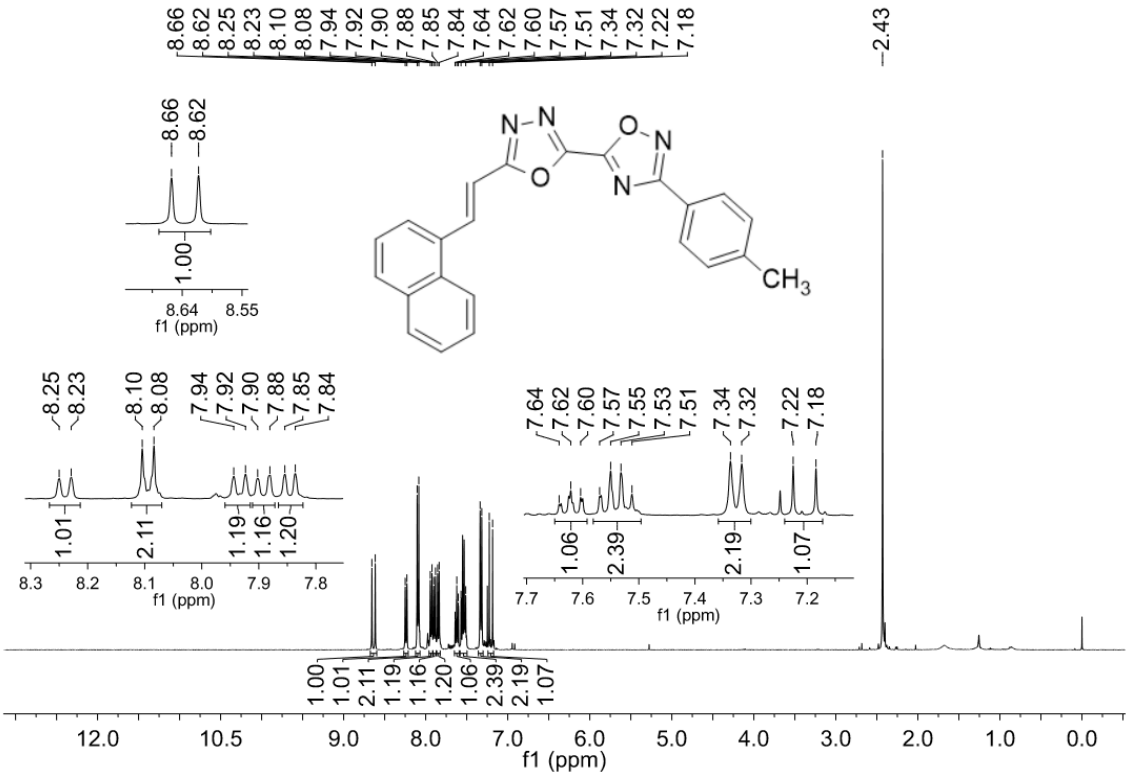

Figure S13. ^{1}H NMR spectrum ($CDCl_3$ at 400 MHz) of compound **7bb**.

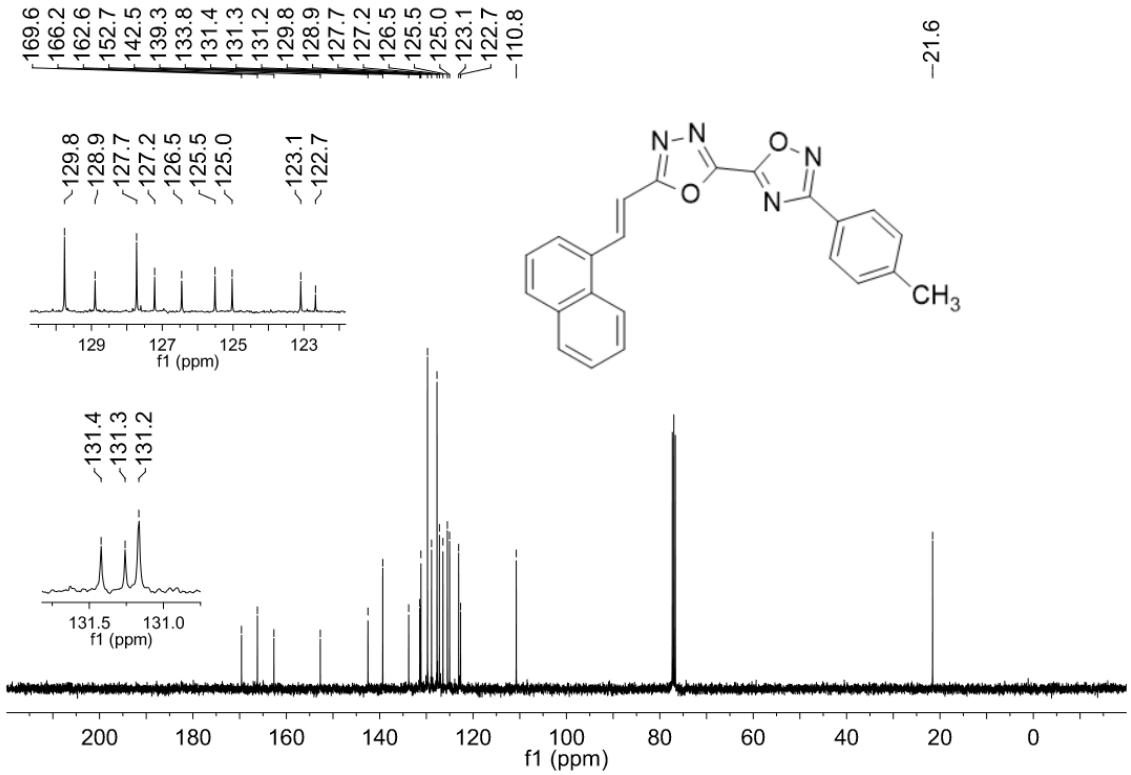

Figure S14. ^{13}C NMR spectrum ($CDCl_3$ at 100 MHz) of compound **7bb**.

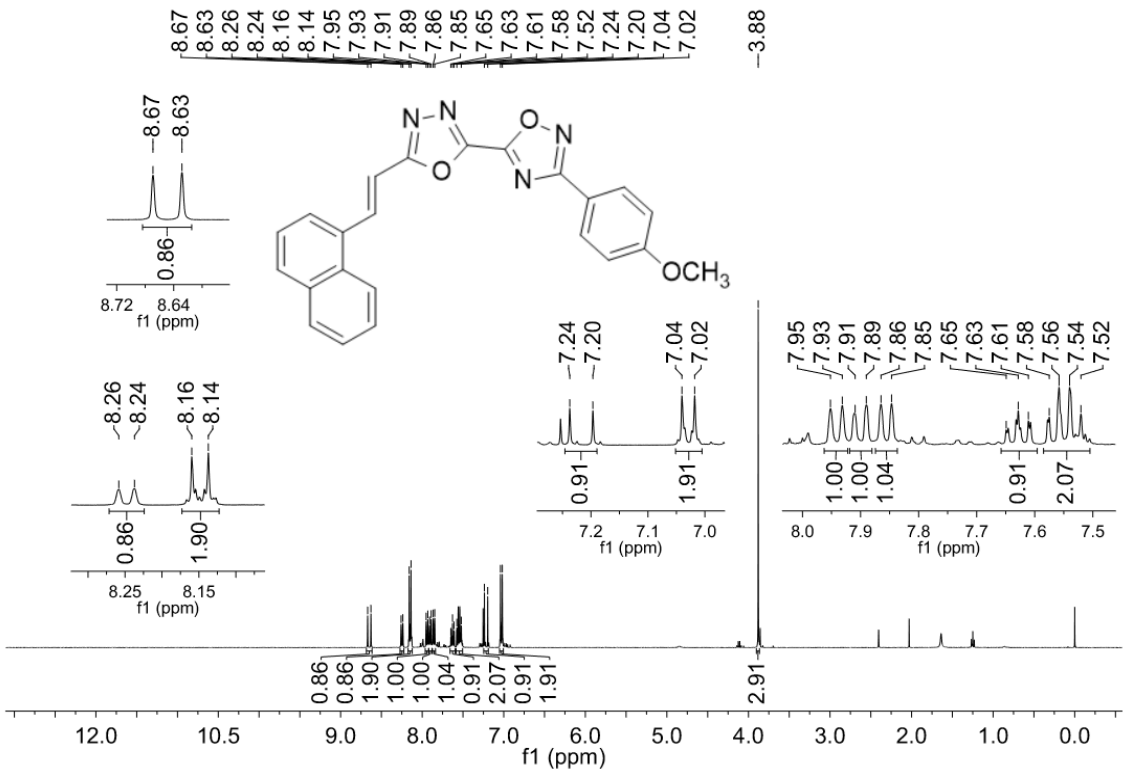

Figure S15. ^{1}H NMR spectrum ($CDCl_3$ at 400 MHz) of compound **7bc**.

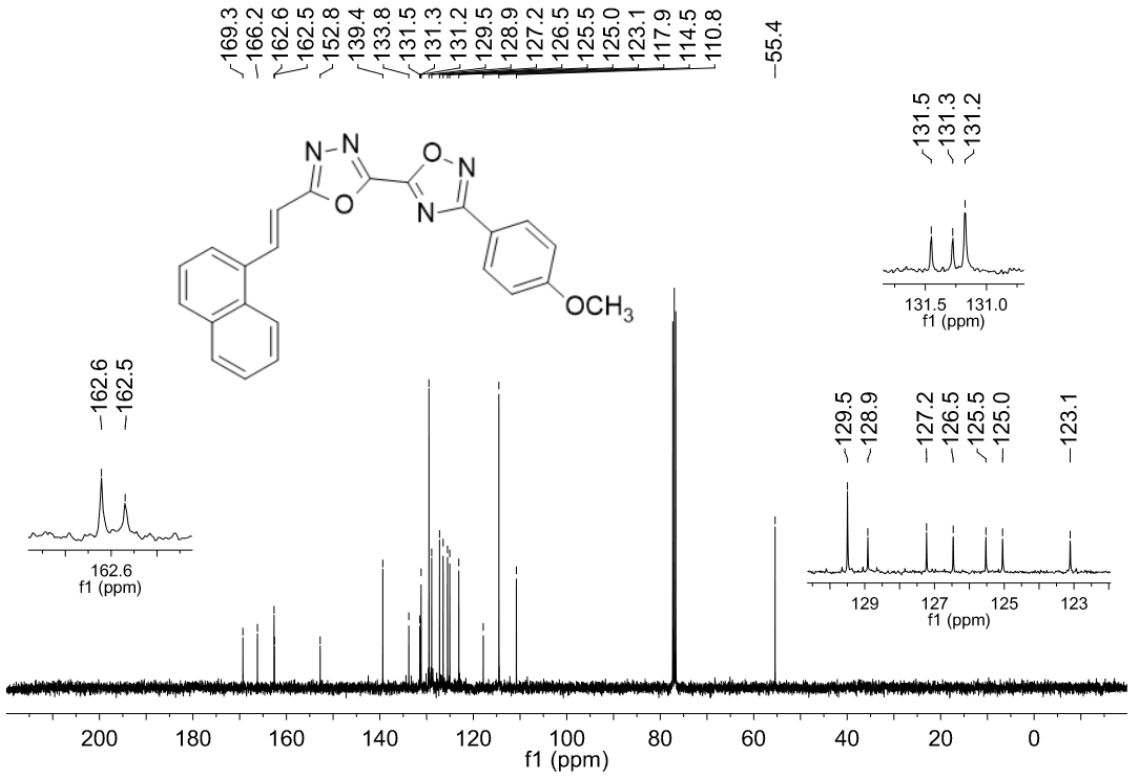

Figure S16. ^{13}C NMR spectrum ($CDCl_3$ at 100 MHz) of compound **7bc**.

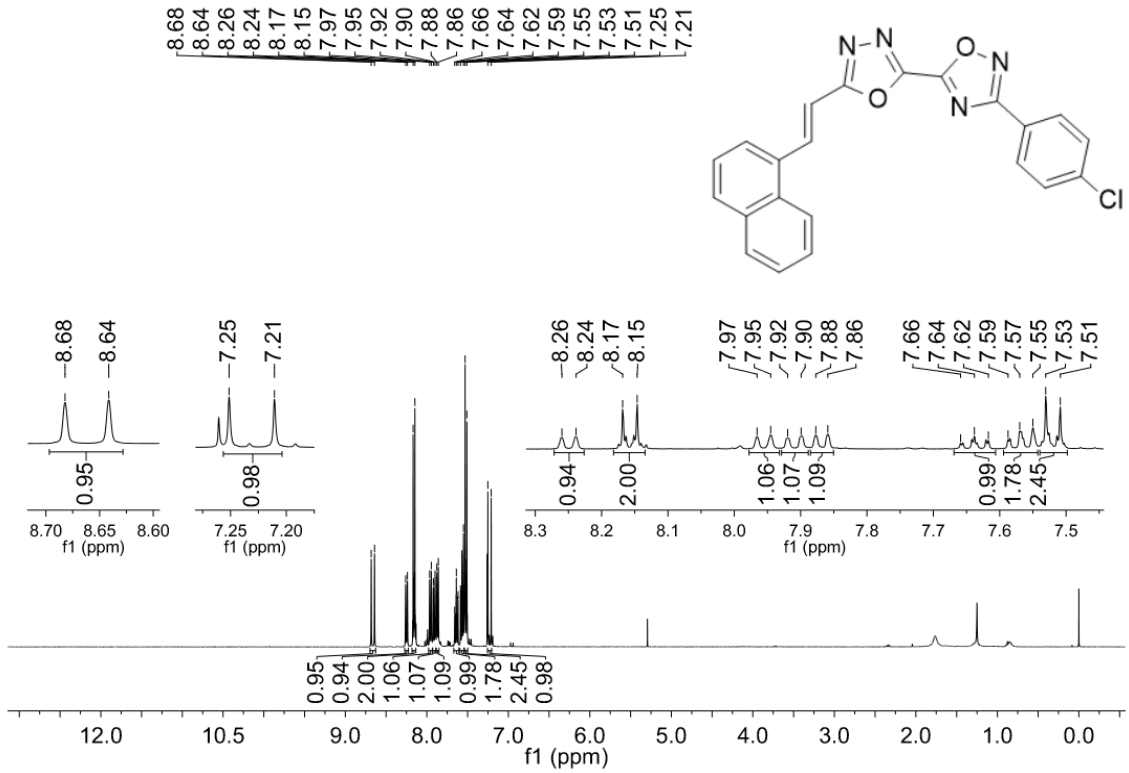

Figure S17. ^{1}H NMR spectrum ($CDCl_3$ at 400 MHz) of compound **7bd**.

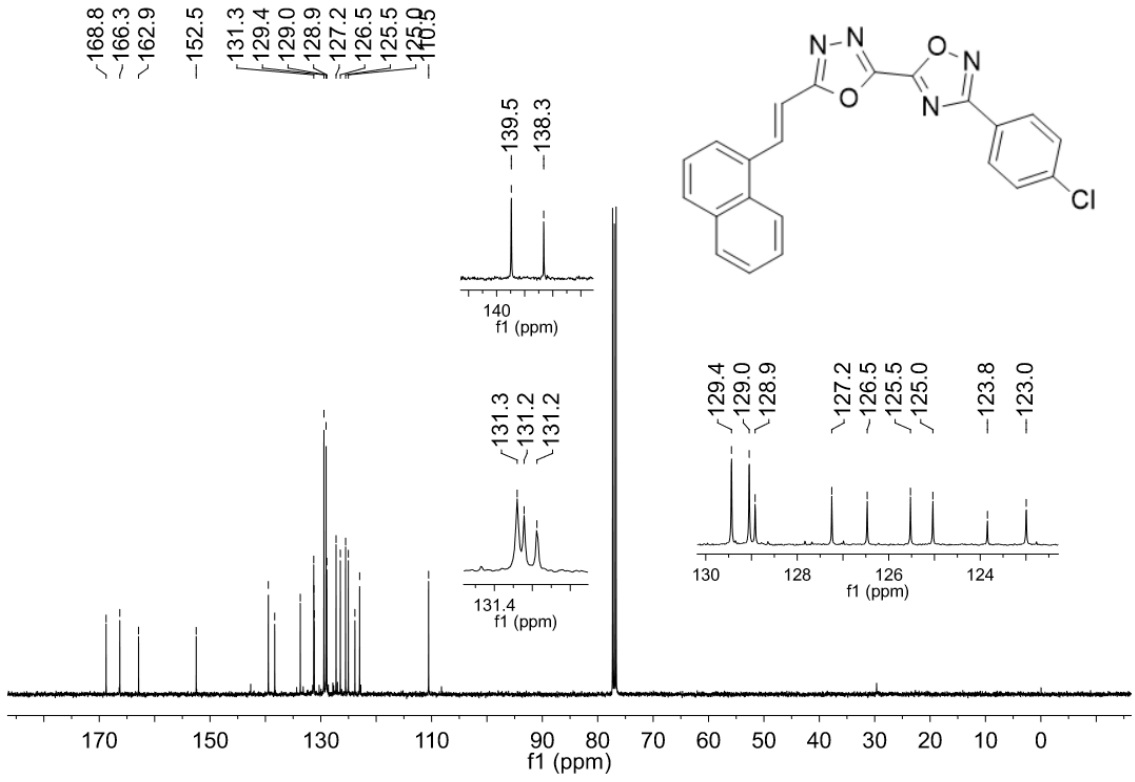

Figure S18. ^{13}C NMR spectrum ($CDCl_3$ at 100 MHz) of compound **7bd**.

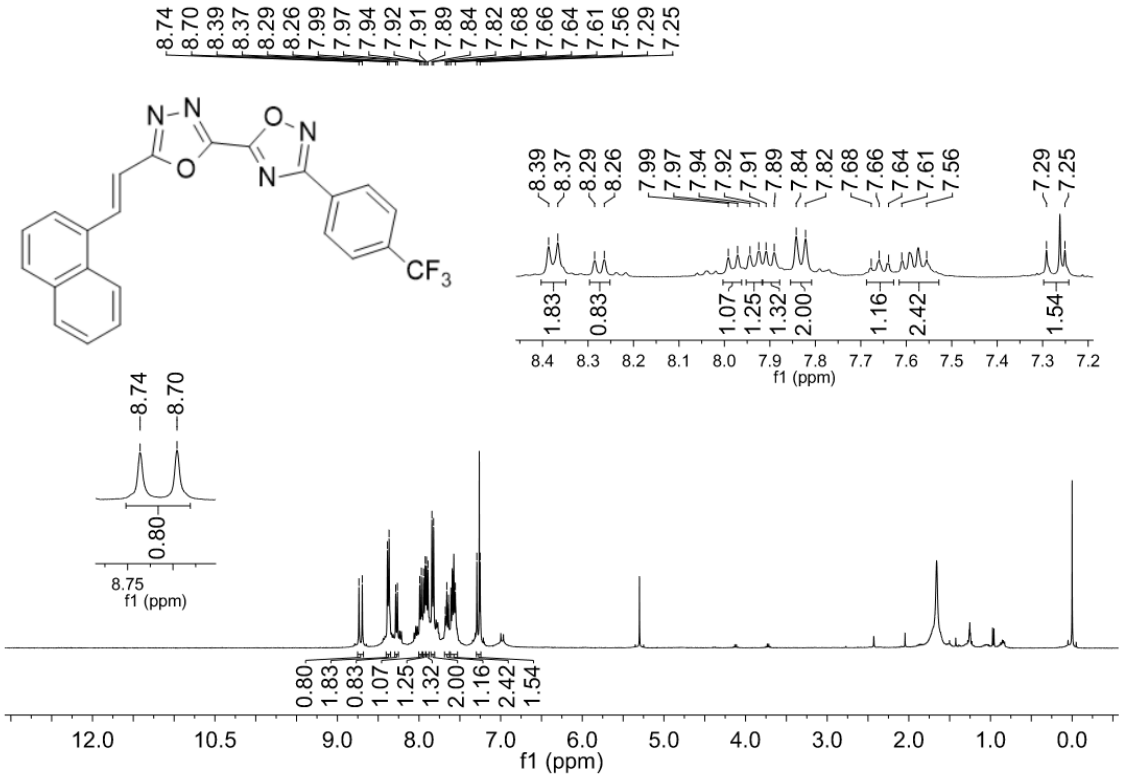

Figure S19. ^{1}H NMR spectrum ($CDCl_3$ at 400 MHz) of compound **7be**.

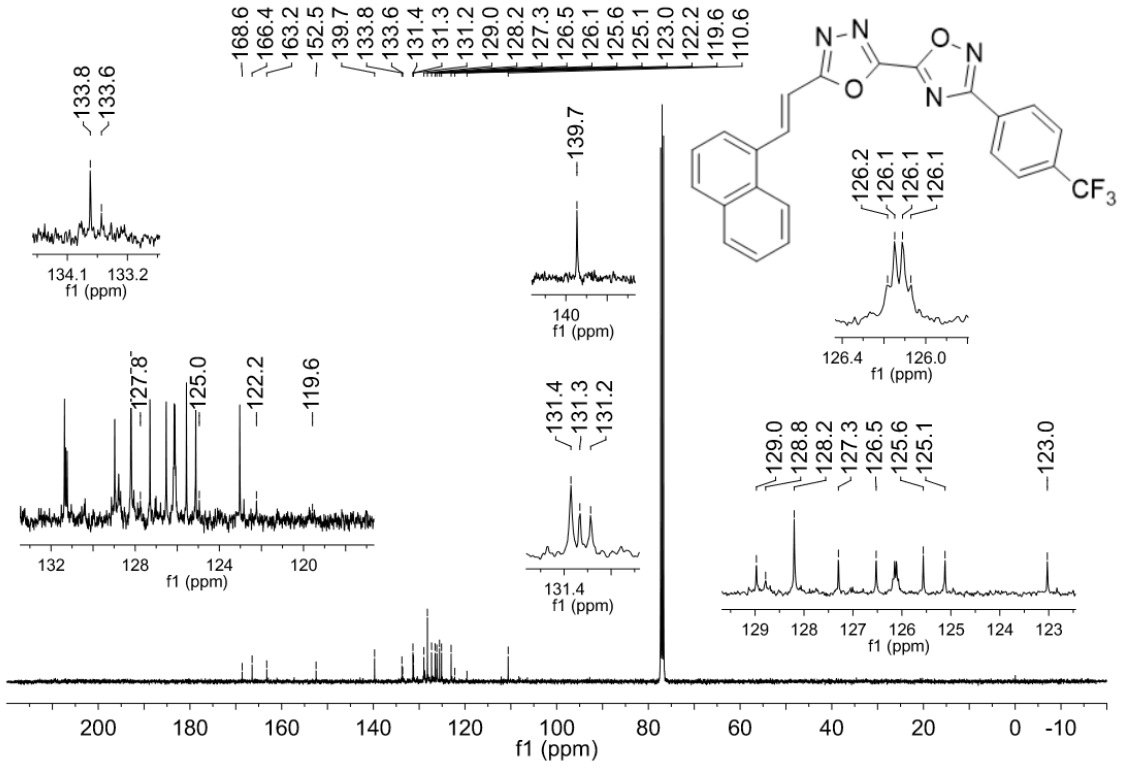

Figure S20. ^{13}C NMR spectrum ($CDCl_3$ at 100 MHz) of compound **7be**.

HRMS Spectra of compounds 7aa-be

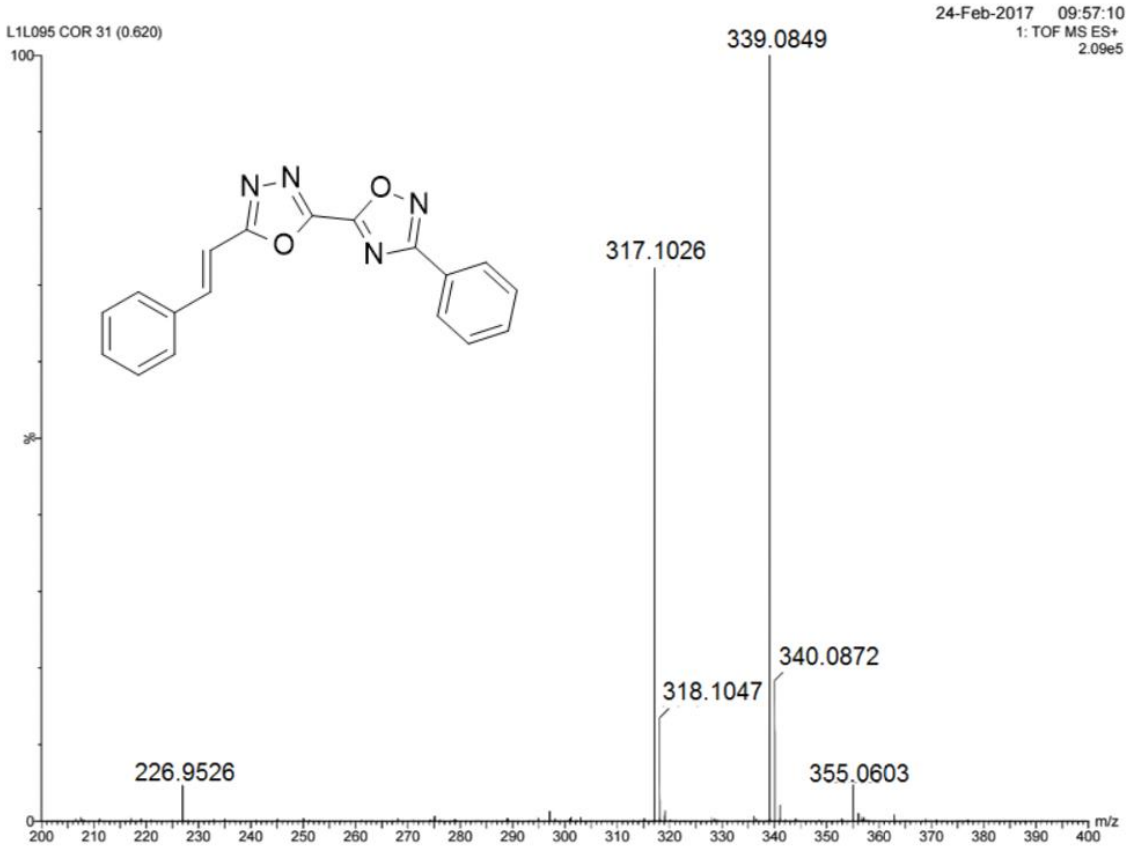

Figure S21. HRMS Spectrum of compound **7aa** (ESI+).

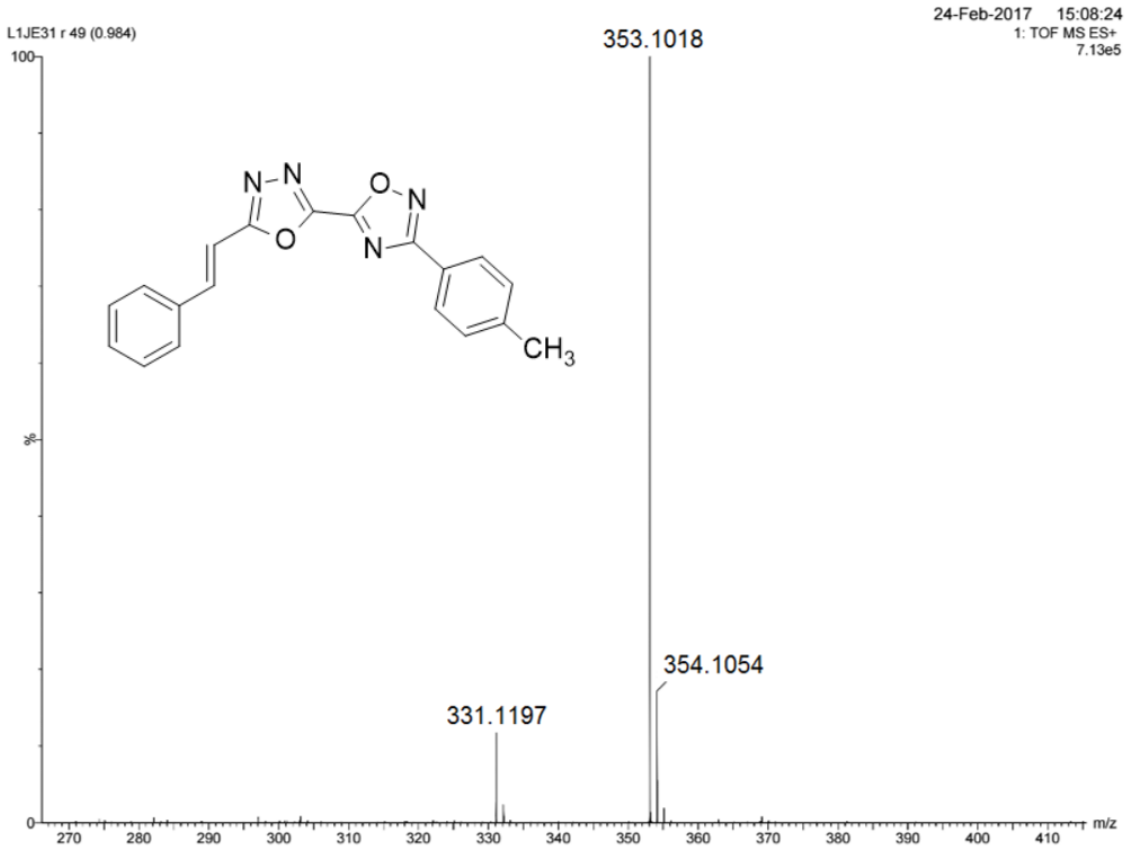

Figure S22. HRMS Spectrum of compound **7ab** (ESI+).

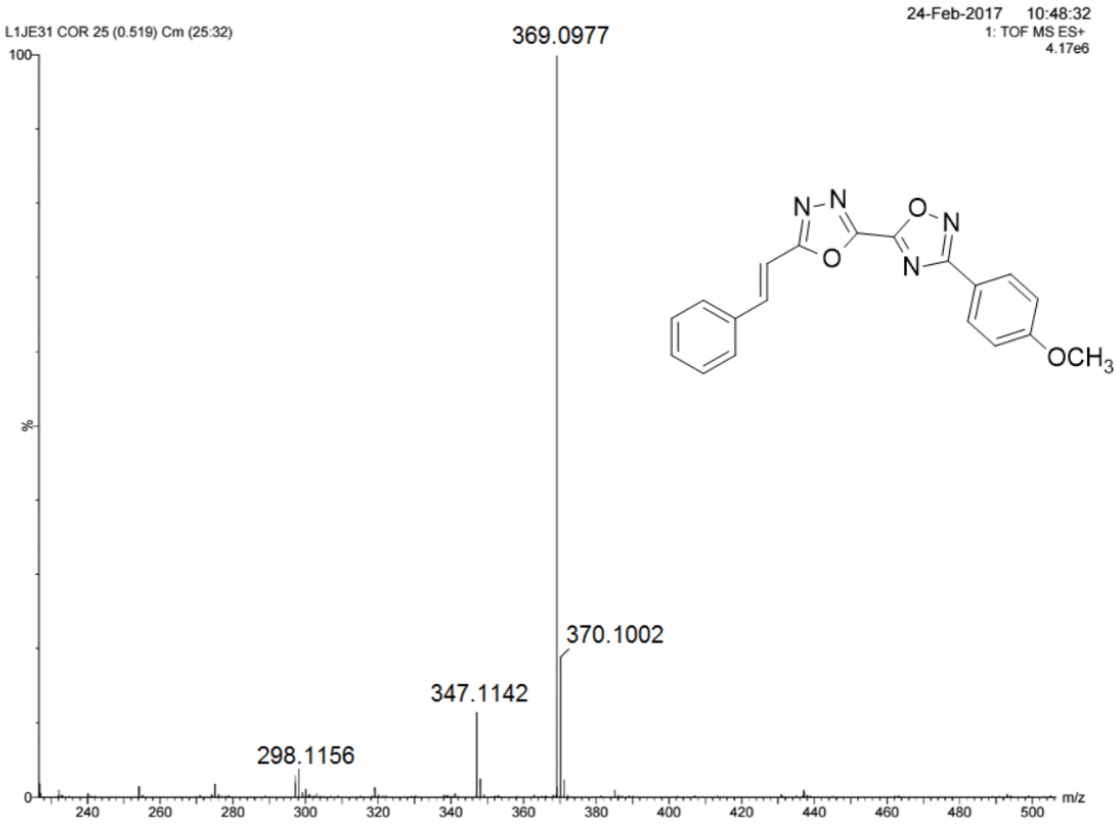

Figure S23. HRMS Spectrum of compound **7ac** (ESI+).

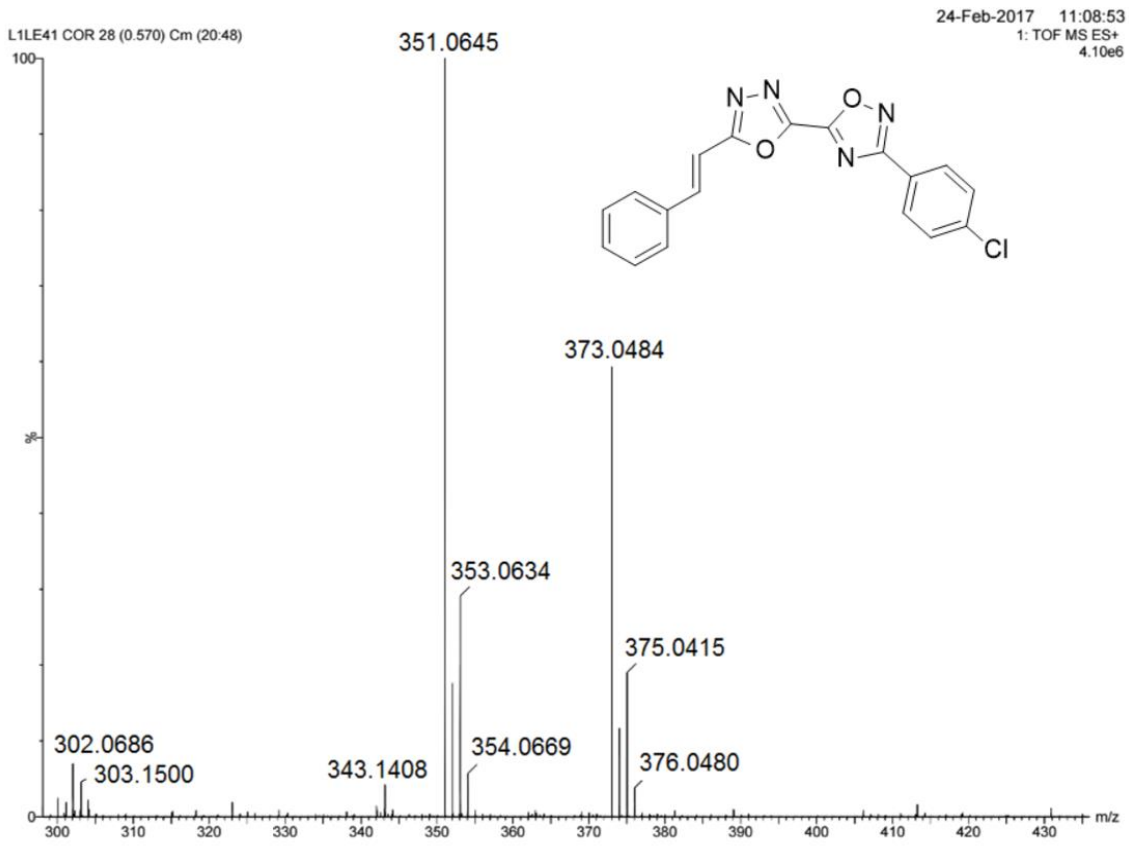

Figure S24. HRMS Spectrum of compound **7ad** (ESI+).

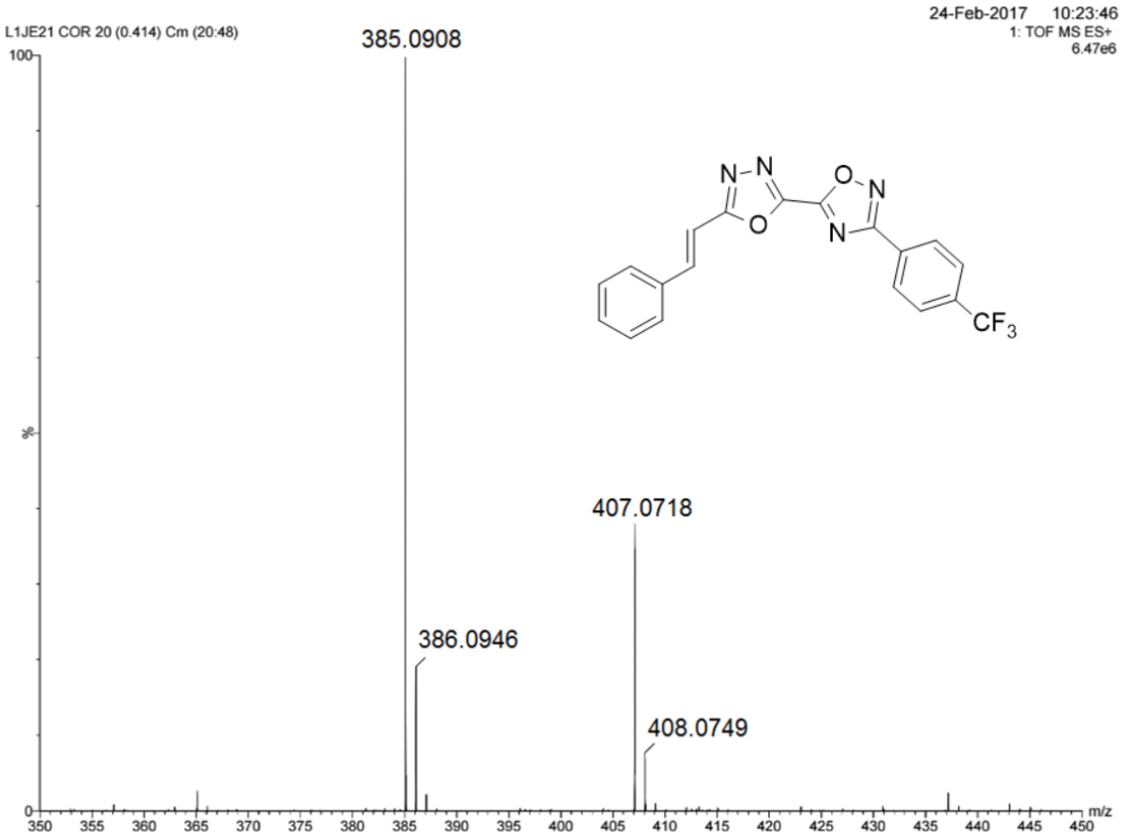

Figure S25. HRMS Spectrum of compound **7ae** (ESI+).

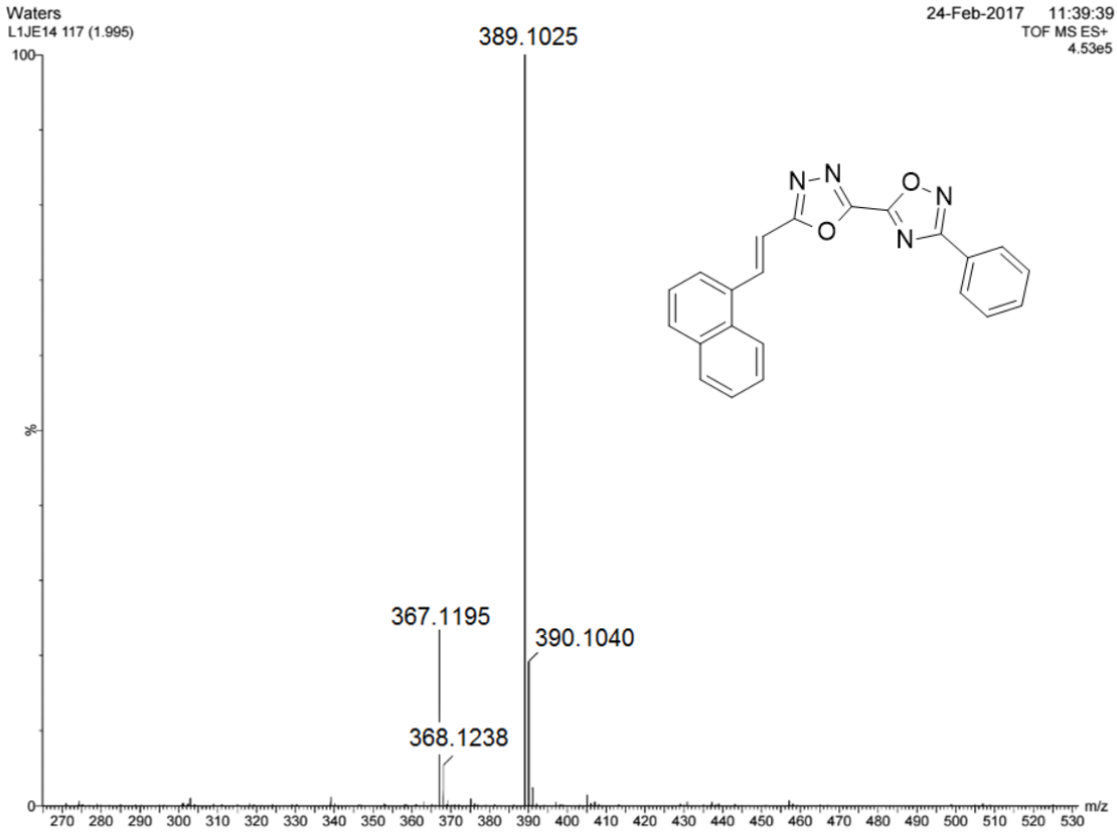

Figure S26. HRMS Spectrum of compound **7ba** (ESI+).

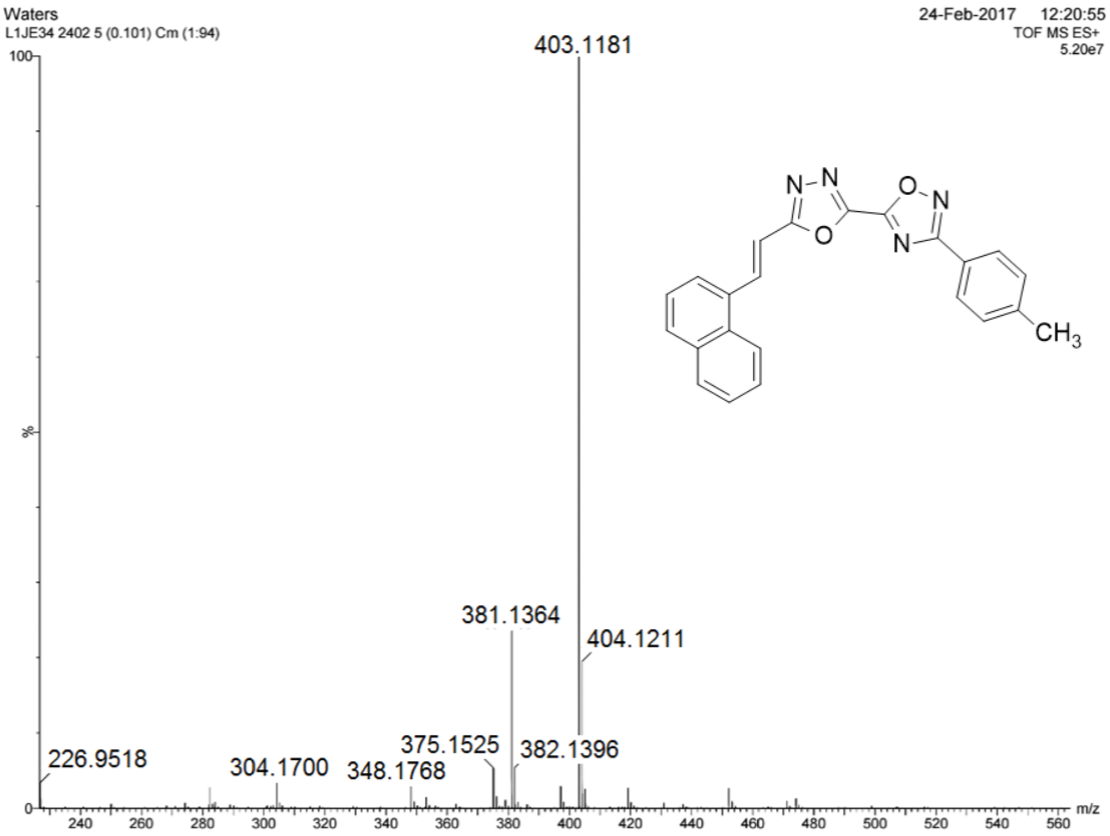

Figure S27. HRMS Spectrum of compound **7bb** (ESI+).

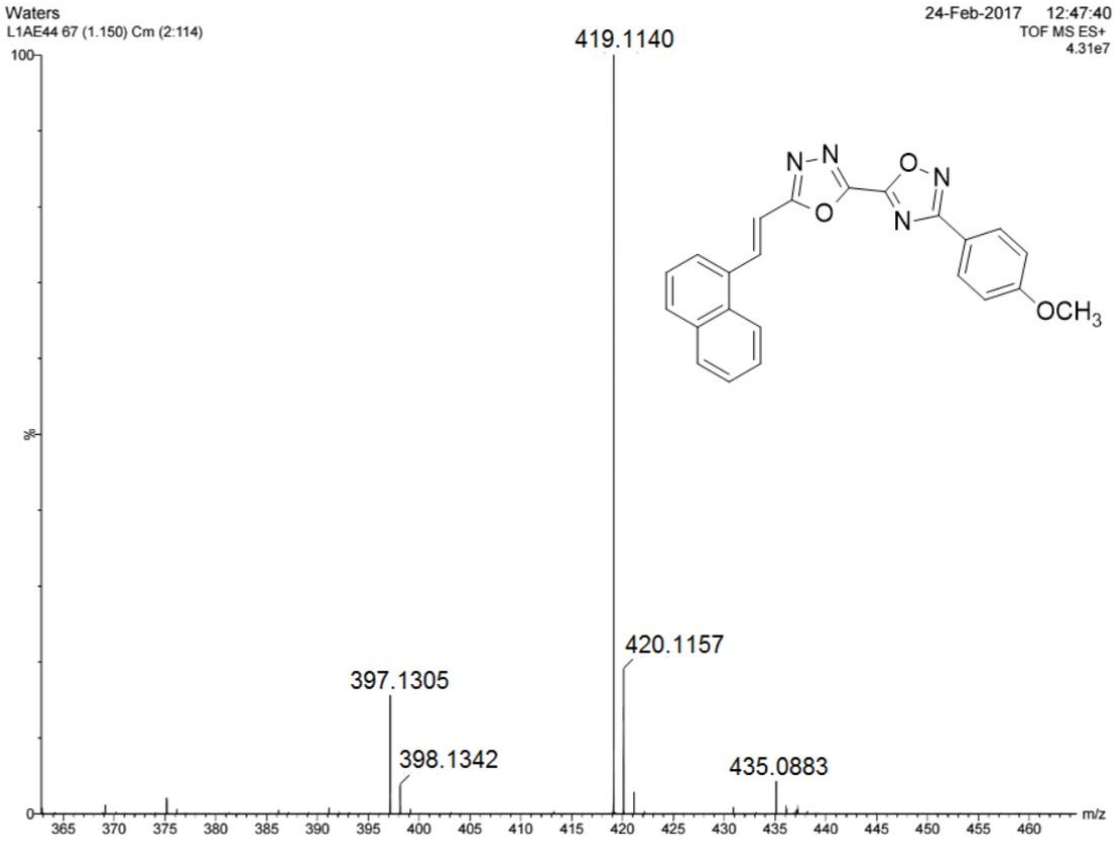

Figure S28. HRMS Spectrum of compound **7bc** (ESI+).

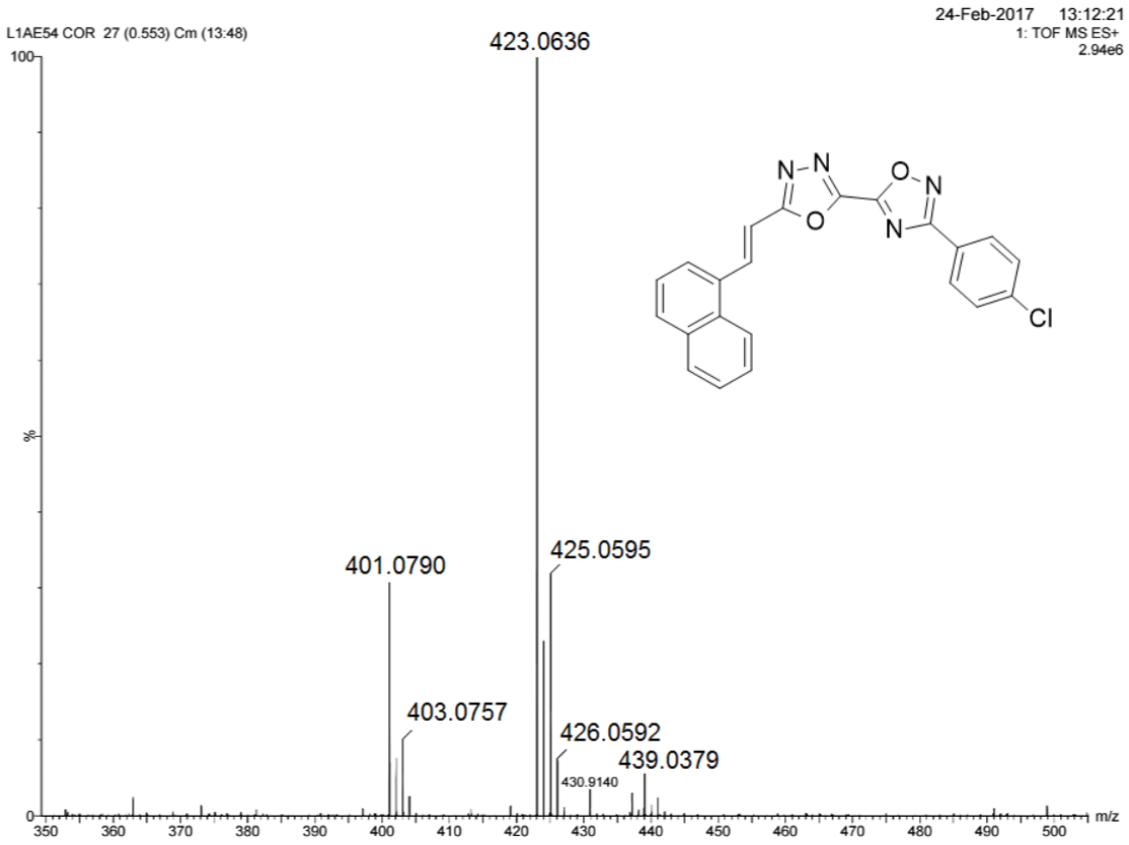

Figure S29. HRMS Spectrum of compound **7bd** (ESI+).

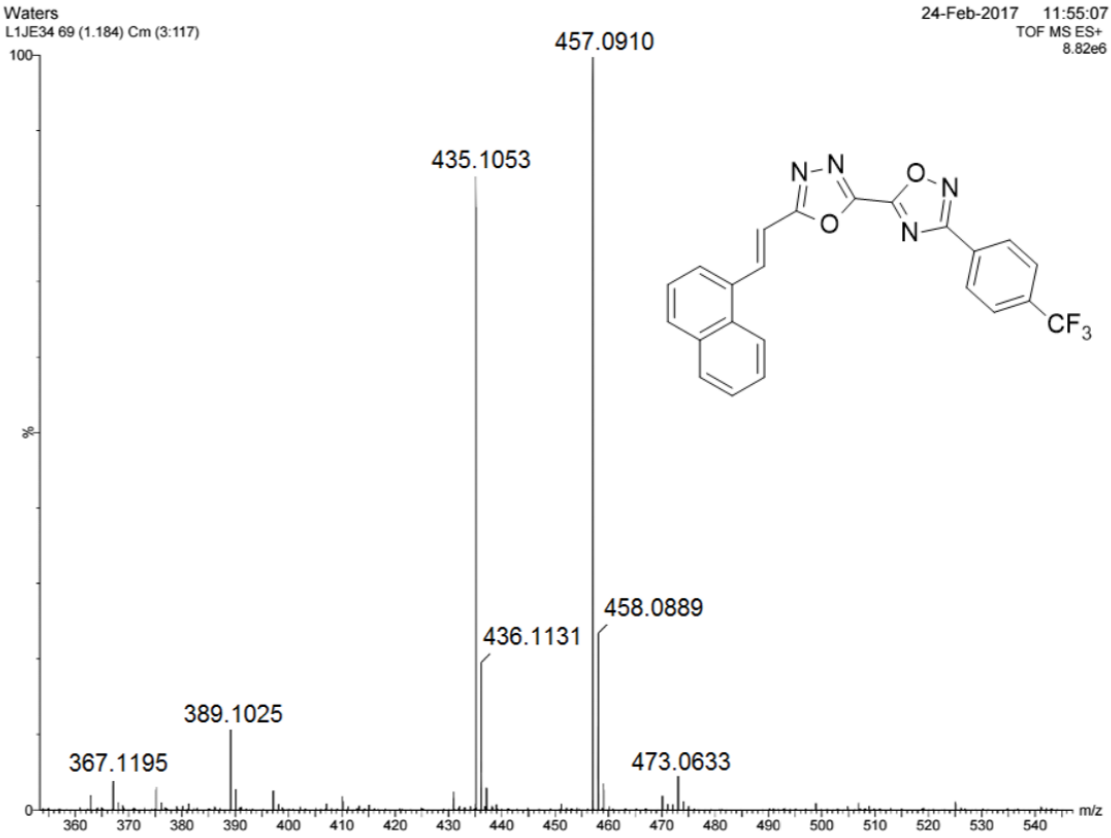

Figure S30. HRMS Spectrum of compound **7be** (ESI+).

Table S1. Crystal data and details of the refinement of the crystal structure of **7aa**.

Compound	**7aa**
Empirical formula	$C_{18}H_{12}N_4O_2$
Formula weight	316.32
Temperature (K)	100(2)
Wavelength	0.71073
Crystal system	Monoclinic
Space group	$P2_1/c$
a(Å)	15.8581(13)
b (Å)	4.2689(3)
c (Å)	22.0230(18)
α (º)	90
β (º)	94.541(3)
γ (º)	90
Volume (Å^3)	1486.2(2)
Z	4
Calculated density(mg·m^{-3})	1.414
Absorp. coefficient (mm^{-1})	0.096
F (000)	656
Crystal size (mm)	0.373 x 0.104 x 0.080
Theta range for data collection (º)	2.34 to 27.13
Limiting indices	$-20 \leq h \leq 20$. $-5 \leq k \leq 5$. $-28 \leq l \leq 28$
Reflections collected / unique	12694 /3290
Completeness to theta	99.8%
Absorption correction	Semi-empirical from equivalents
Max. and min. trans.	0.8620/0.6741
Data / restraints / parameters	3290 / 0 / 217
Goodness-of-fit on F^2	1.015
ÍndiceR_{int}	0.0768
Final R indices R_1 and $wR_2[I>2\sigma(I)]$	0.0572 /0.01129
R indices (all data)	0.01129 / 0.01344
Largest diff. peak and hole	0.243 and -0.333 e·A^{-3}

Table S2. Bond lengths [A] and angles [deg] for **7aa**.

O(12)-C(13)	1.364(2)
O(12)-C(16)	1.374(2)
O(1)-C(5)	1.346(2)
O(1)-N(2)	1.413(2)
N(15)-C(16)	1.302(3)
N(15)-N(14)	1.402(2)
N(14)-C(13)	1.286(3)
N(2)-C(3)	1.310(3)
N(4)-C(5)	1.290(3)
N(4)-C(3)	1.392(2)
C(13)-C(5)	1.444(3)
C(6)-C(11)	1.384(3)
C(6)-C(7)	1.402(3)
C(6)-C(3)	1.460(3)
C(19)-C(20)	1.388(3)
C(19)-C(24)	1.397(3)
C(19)-C(18)	1.472(3)
C(17)-C(18)	1.339(3)
C(17)-C(16)	1.437(3)
C(8)-C(9)	1.378(3)
C(8)-C(7)	1.382(3)
C(10)-C(11)	1.384(3)
C(10)-C(9)	1.392(3)
C(20)-C(21)	1.389(3)
C(21)-C(22)	1.375(4)
C(22)-C(23)	1.382(4)
C(24)-C(23)	1.382(3)
C(13)-O(12)-C(16)	101.45(16)
C(5)-O(1)-N(2)	104.81(16)
C(16)-N(15)-N(14)	106.42(18)
C(13)-N(14)-N(15)	105.77(17)
C(3)-N(2)-O(1)	104.41(16)
C(5)-N(4)-C(3)	101.83(17)
N(14)-C(13)-O(12)	113.99(18)
N(14)-C(13)-C(5)	126.46(19)
O(12)-C(13)-C(5)	119.49(19)
C(11)-C(6)-C(7)	119.6(2)
C(11)-C(6)-C(3)	121.18(18)
C(7)-C(6)-C(3)	119.2(2)
C(20)-C(19)-C(24)	118.7(2)
C(20)-C(19)-C(18)	118.7(2)
C(24)-C(19)-C(18)	122.6(2)
N(4)-C(5)-O(1)	115.14(18)
N(4)-C(5)-C(13)	129.97(19)
O(1)-C(5)-C(13)	114.87(19)
C(18)-C(17)-C(16)	124.0(2)

C(17)-C(18)-C(19)	125.4(2)
N(2)-C(3)-N(4)	113.8(2)
N(2)-C(3)-C(6)	121.88(18)
N(4)-C(3)-C(6)	124.29(19)
N(15)-C(16)-O(12)	112.36(17)
N(15)-C(16)-C(17)	126.9(2)
O(12)-C(16)-C(17)	120.75(19)
C(9)-C(8)-C(7)	119.98(19)
C(8)-C(7)-C(6)	120.1(2)
C(11)-C(10)-C(9)	120.0(2)
C(19)-C(20)-C(21)	121.1(2)
C(8)-C(9)-C(10)	120.3(2)
C(10)-C(11)-C(6)	120.09(18)
C(22)-C(21)-C(20)	119.6(2)
C(21)-C(22)-C(23)	120.1(2)
C(23)-C(24)-C(19)	120.0(2)
C(22)-C(23)-C(24)	120.6(2)

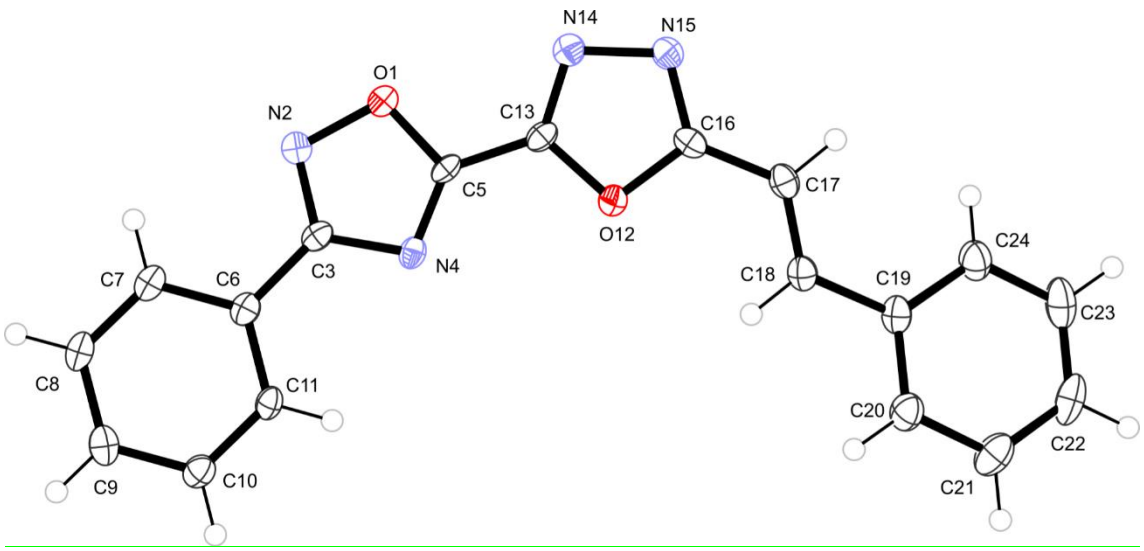

Figure S31. Projection of the molecular structure of the **7aa** ligand. Thermal ellipsoids with 50% probability level.

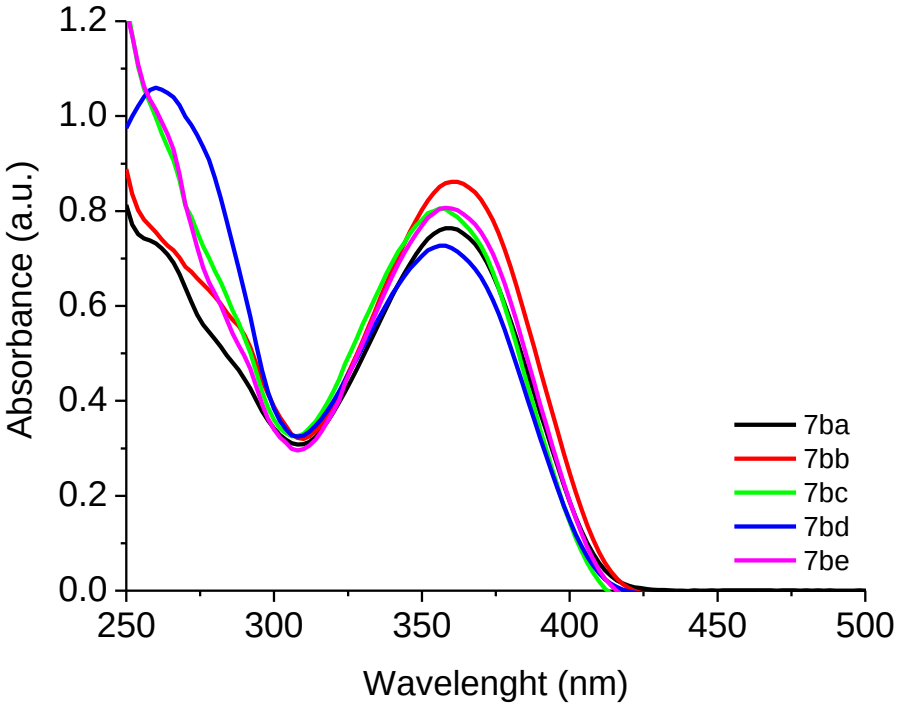

Figure S32. UV-Vis absorption spectra of derivatives **7ba-be** in $CHCl_3$ solution ([ ] = 2.00 x 10^{-5} M).

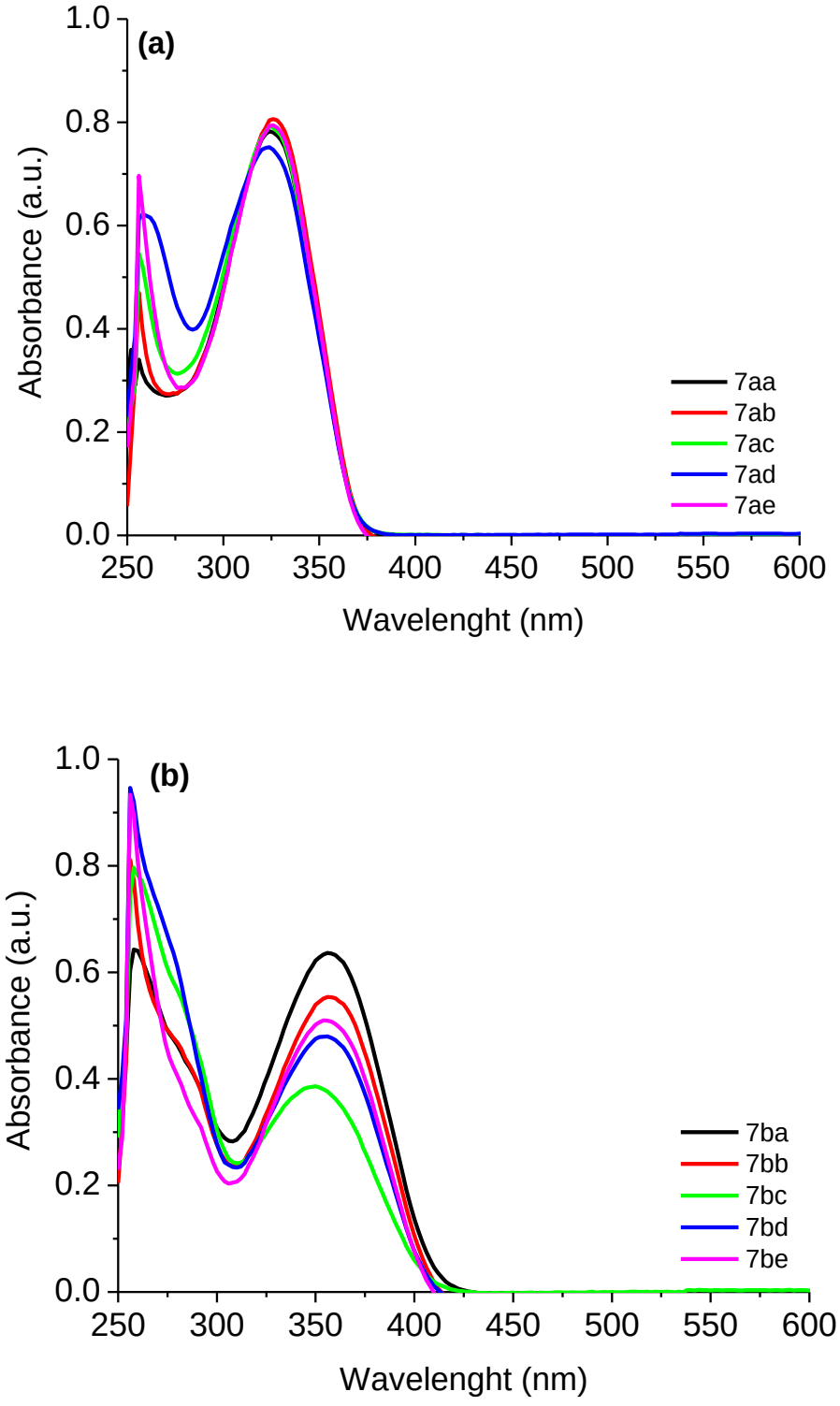

Figure S33. UV-Vis absorption spectra of derivatives **(a) 7aa-ae** and **(b) 7ba-be** in DMSO solution ([ ] = 2.00 x 10^{-5} M).

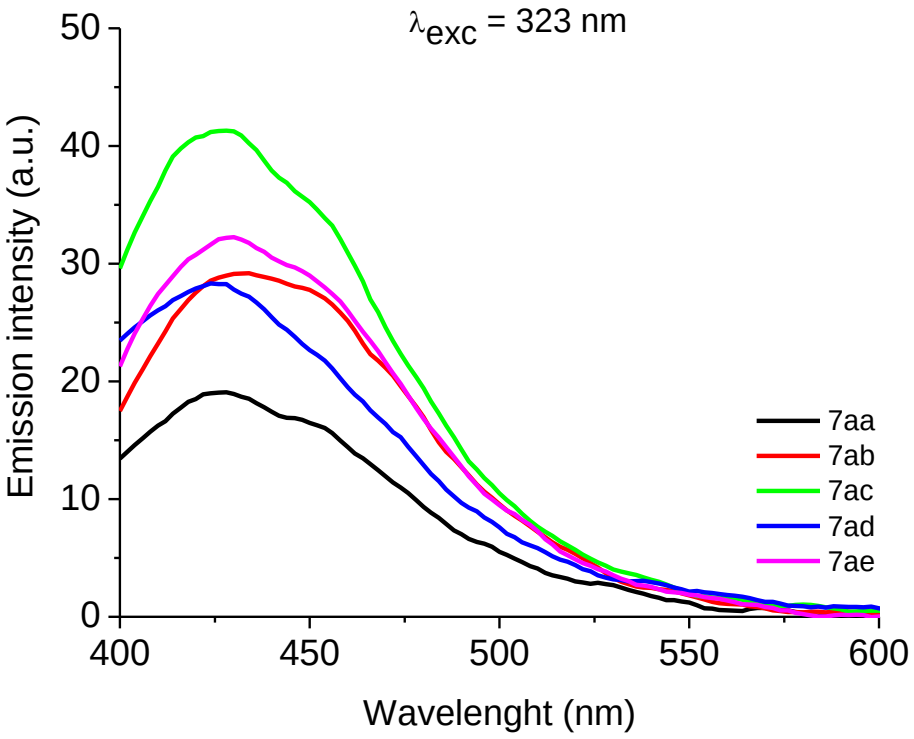

Figure S34. Steady-state emission spectra of derivatives **7aa-ae** (λ_{exc} = 323 nm) in saturated argon chloroform solution ([ ] = 1.00 x 10^{-6} M).

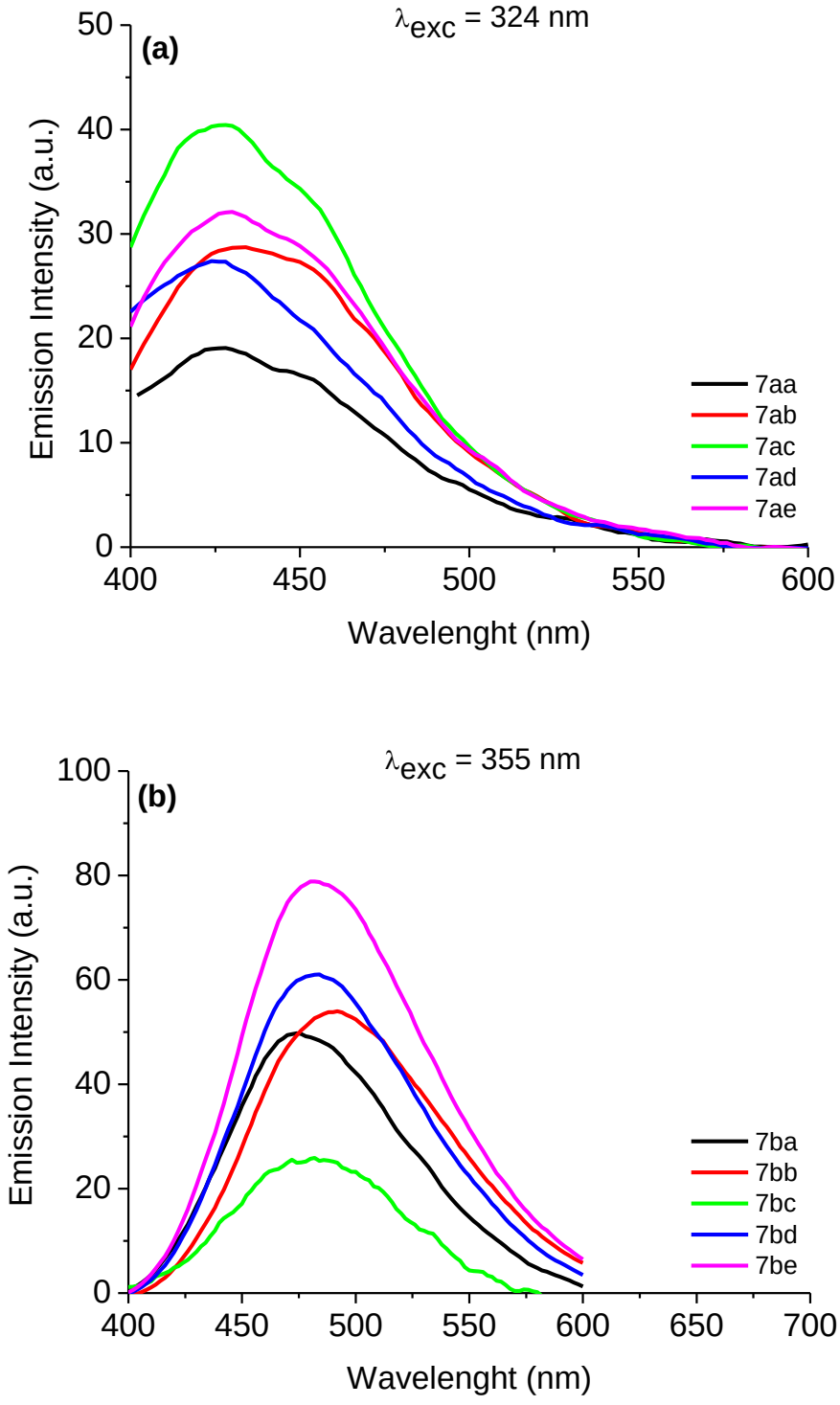

Figure S35. Steady-state emission spectra of derivatives **(a) 7aa-ae** (λ_{exc} = 324 nm) and **(b) 7ba-be** (λ_{exc} = 355 nm) in saturated argon DMSO solution ([ ] = 1.00 x 10^{-6} M).

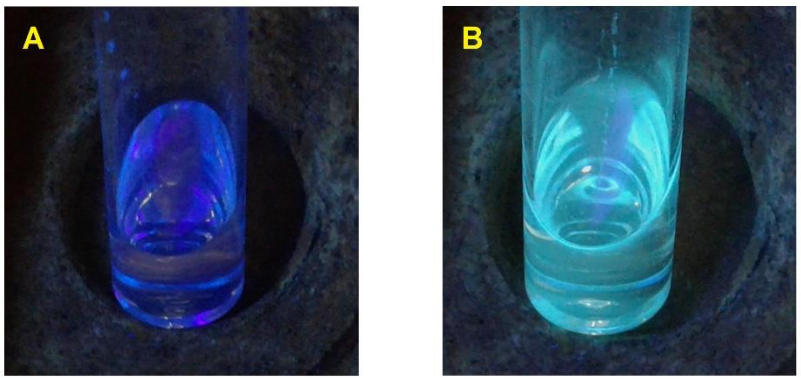

Figure S36. Representative samples of compound **7aa** at 1.0 mg/mL (1.05 x 10^{-3} M) solution in DMSO (**A**), and compound **7ba** at 1.0 mg/mL (9.10 x 10^{-4} M) solution in DMSO (**B**), both under UV illumination (365 nm).

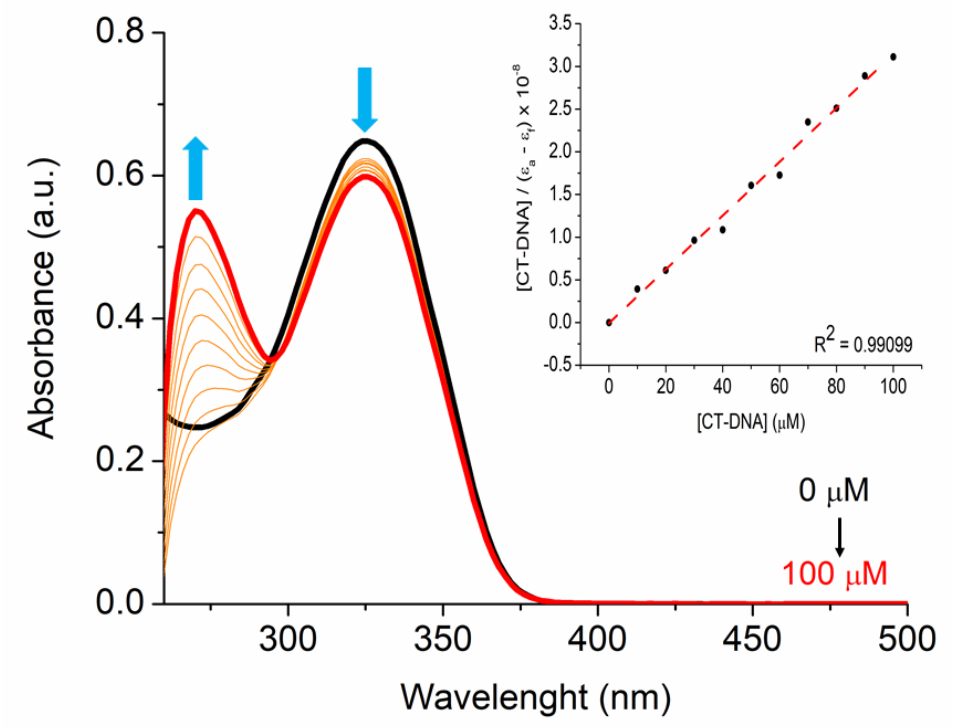

Figure S37. UV-Vis titration absorption spectra of derivative **7ab**, in a DMSO (2%)/Tris-HCl buffer (pH 7.2) solution. The concentration of CT-DNA ranged from 0 to 100 μM. Insert graph shows the plot of [DNA]/($\varepsilon_a - \varepsilon_f$) *versus* [DNA].

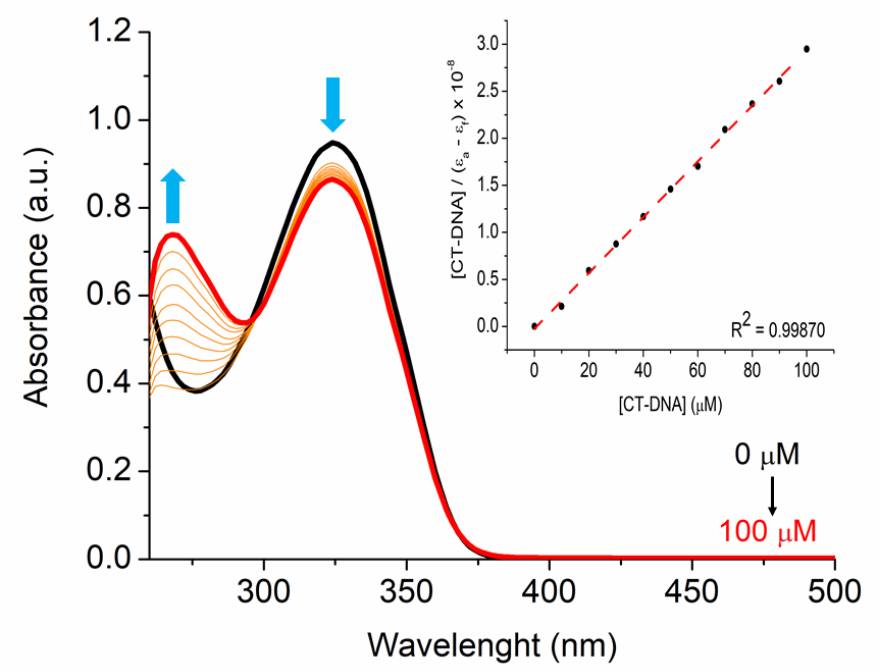

Figure S38. UV-Vis titration absorption spectra of derivative **7ac**, in a DMSO (2%)/Tris-HCl buffer (pH 7.2) solution. The concentration of CT-DNA ranged from 0 to 100 μM. Insert graph shows the plot of [DNA]/($\varepsilon_a - \varepsilon_f$) *versus* [DNA].

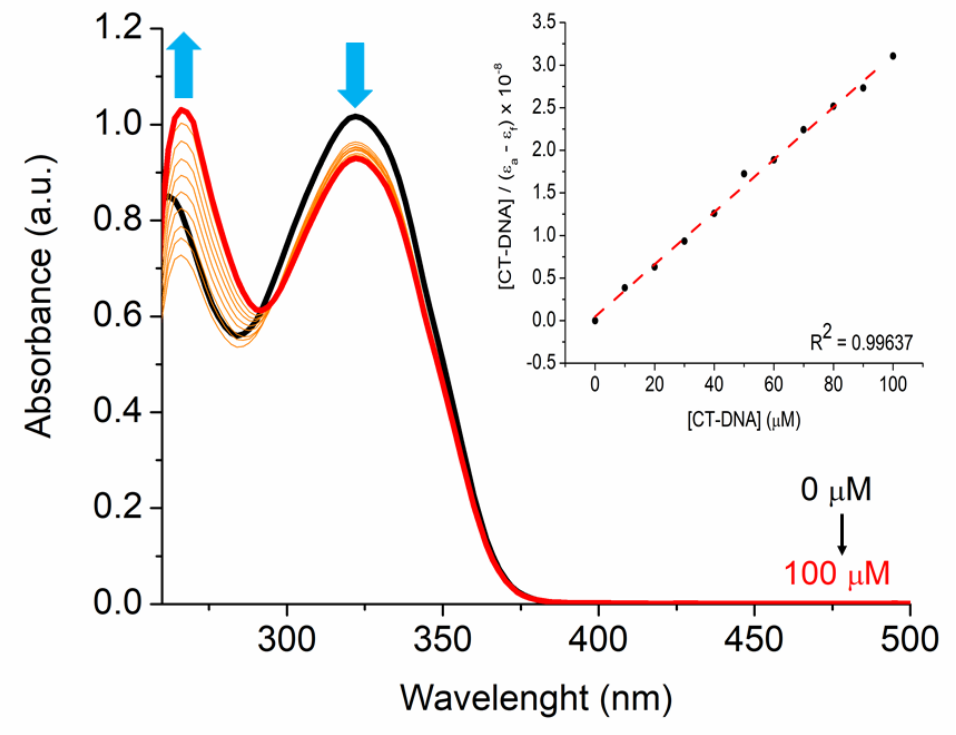

Figure S39. UV-Vis titration absorption spectra of derivative **7ad**, in a DMSO (2%)/Tris-HCl buffer (pH 7.2) solution. The concentration of CT-DNA ranged from 0 to 100 μM. Insert graph shows the plot of [DNA]/($\varepsilon_a - \varepsilon_f$) *versus* [DNA].

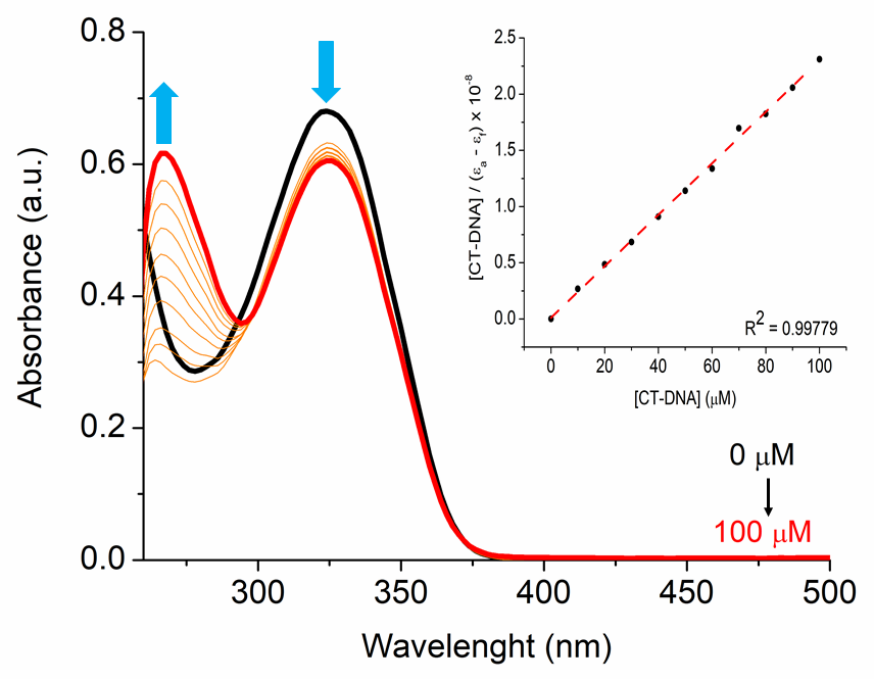

Figure S40. UV-Vis titration absorption spectra of derivative **7ae**, in a DMSO (2%)/Tris-HCl buffer (pH 7.2) solution. The concentration of CT-DNA ranged from 0 to 100 μM. Insert graph shows the plot of [DNA]/($\varepsilon_a - \varepsilon_f$) *versus* [DNA].

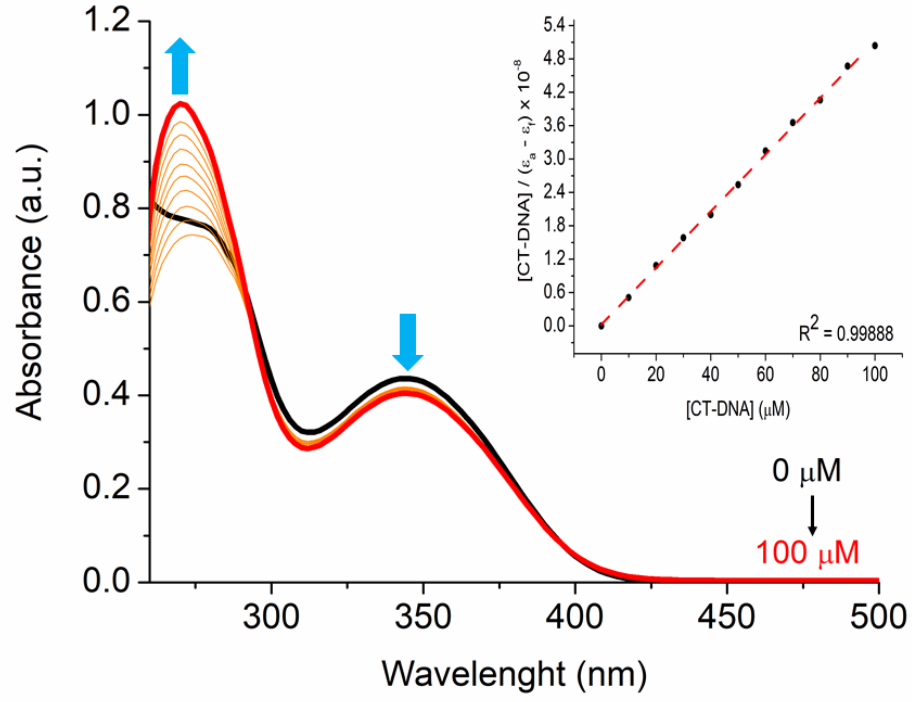

Figure S41. UV-Vis titration absorption spectra of derivative **7bb**, in a DMSO (2%)/Tris-HCl buffer (pH 7.2) solution. The concentration of CT-DNA ranged from 0 to 100 μM. Insert graph shows the plot of [DNA]/($\varepsilon_a - \varepsilon_f$) *versus* [DNA].

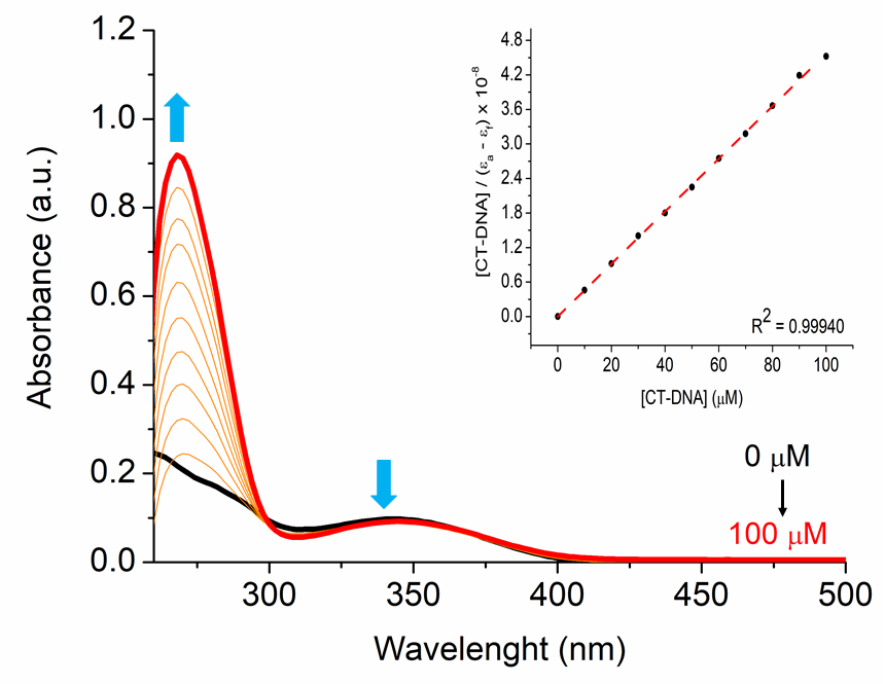

Figure S42. UV-Vis titration absorption spectra of derivative **7bc**, in a DMSO (2%)/Tris-HCl buffer (pH 7.2) solution. The concentration of CT-DNA ranged from 0 to 100 μM. Insert graph shows the plot of [DNA]/($\varepsilon_a - \varepsilon_f$) *versus* [DNA].

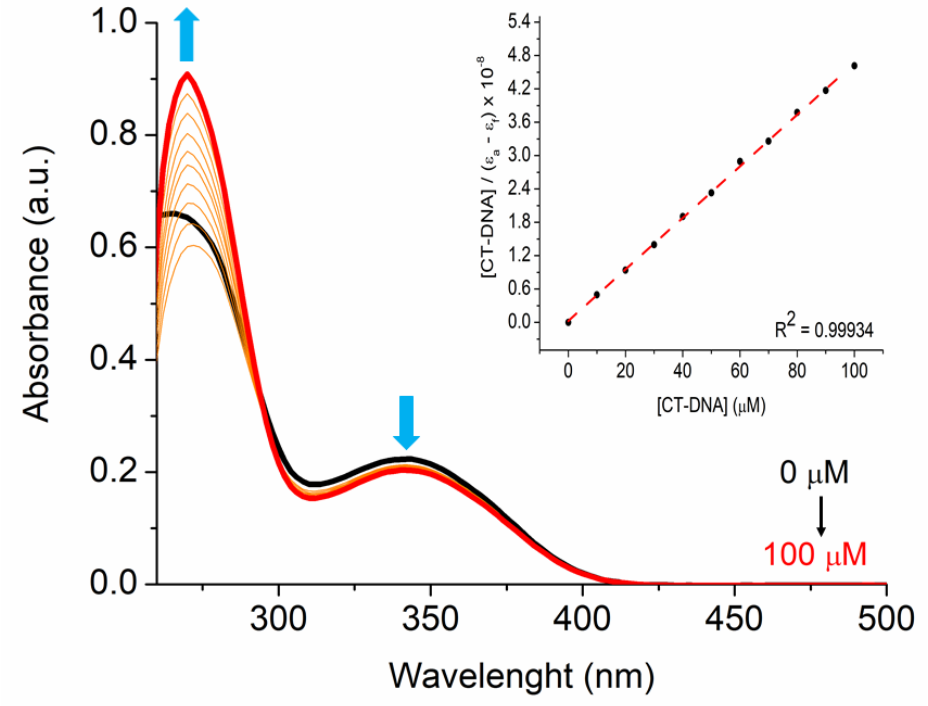

Figure S43. UV-Vis titration absorption spectra of derivative **7bd**, in a DMSO (2%)/Tris-HCl buffer (pH 7.2) solution. The concentration of CT-DNA ranged from 0 to 100 μM. Insert graph shows the plot of [DNA]/($\varepsilon_a - \varepsilon_f$) *versus* [DNA].

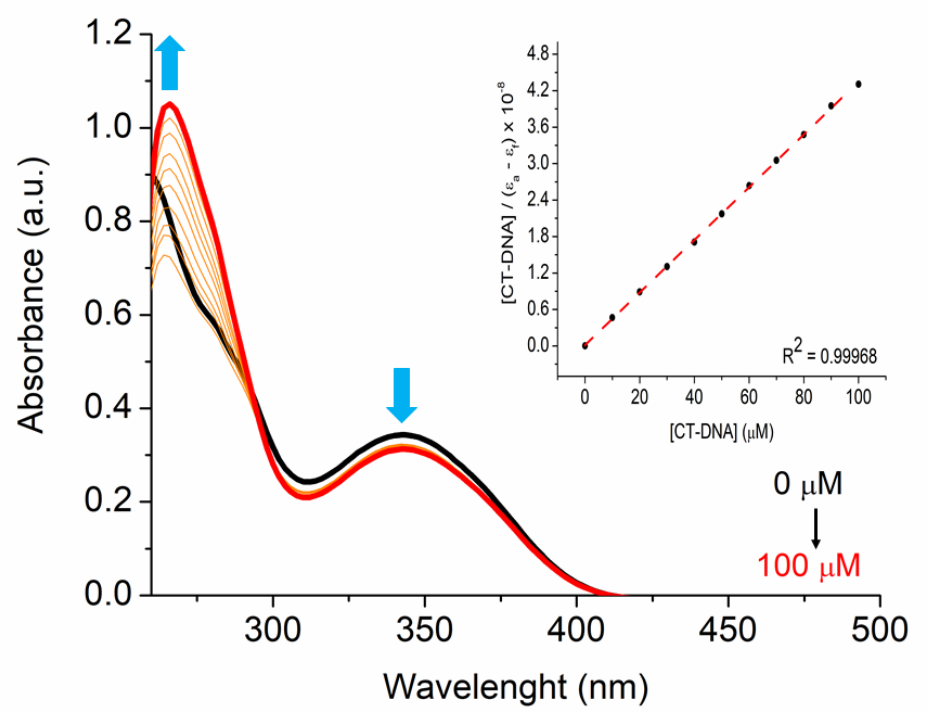

Figure S44. UV-Vis titration absorption spectra of derivative **7be**, in a DMSO (2%)/Tris-HCl buffer (pH 7.2) solution. The concentration of CT-DNA ranged from 0 to 100 μM. Insert graph shows the plot of [DNA]/($\varepsilon_a - \varepsilon_f$) *versus* [DNA].

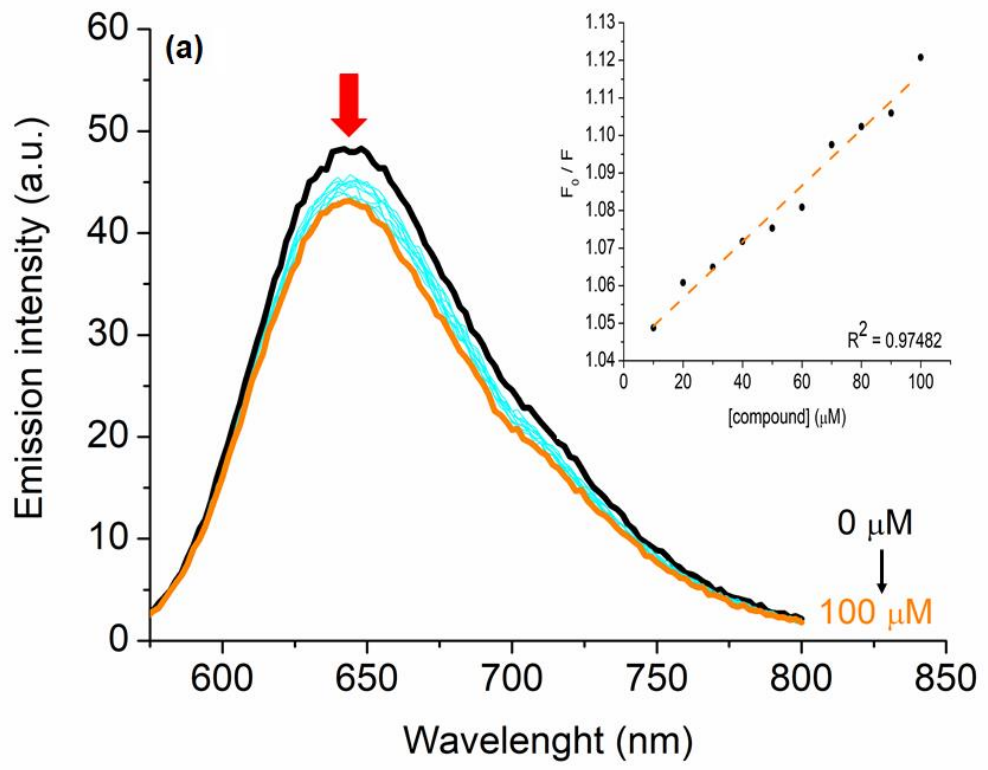

Figure S45. Competitive emission spectra of EB-DNA with derivative **7aa** in a DMSO (2%)/Tris-HCl buffer (pH 7.2) solution. The concentration of compound ranged from 0 to 100 μM. Insert graph shows the plot of F_0/F *versus* [compound].

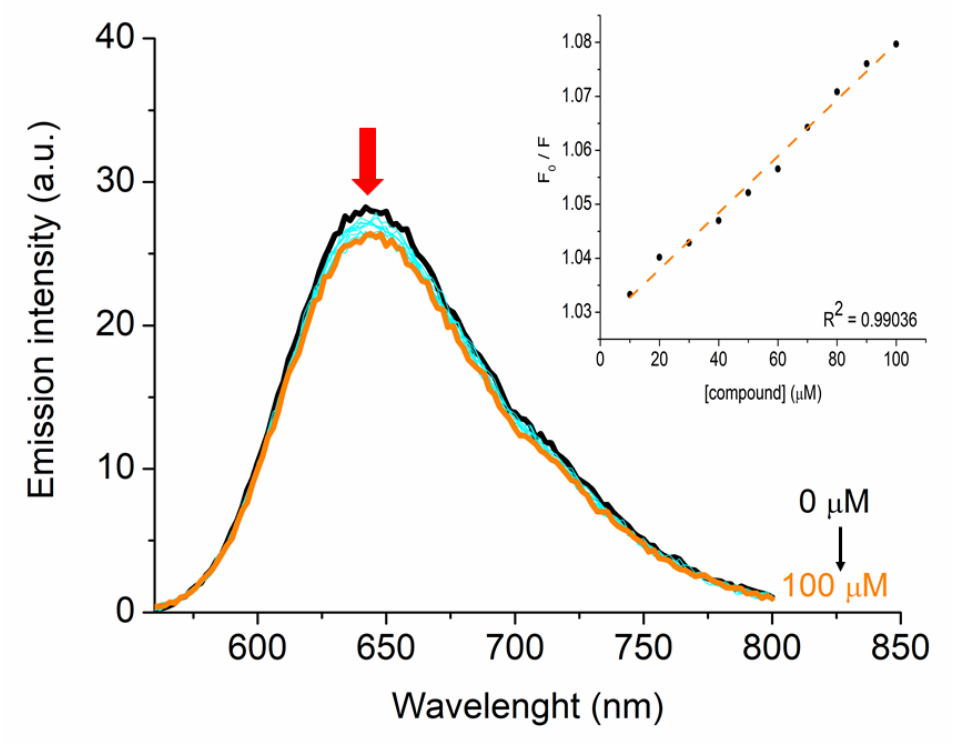

Figure S46. Competitive emission spectra of EB-DNA with derivative **7ab** in a DMSO (2%)/Tris-HCl buffer (pH 7.2) solution. The concentration of compound ranged from 0 to 100 μM. Insert graph shows the plot of F_0/F *versus* [compound].

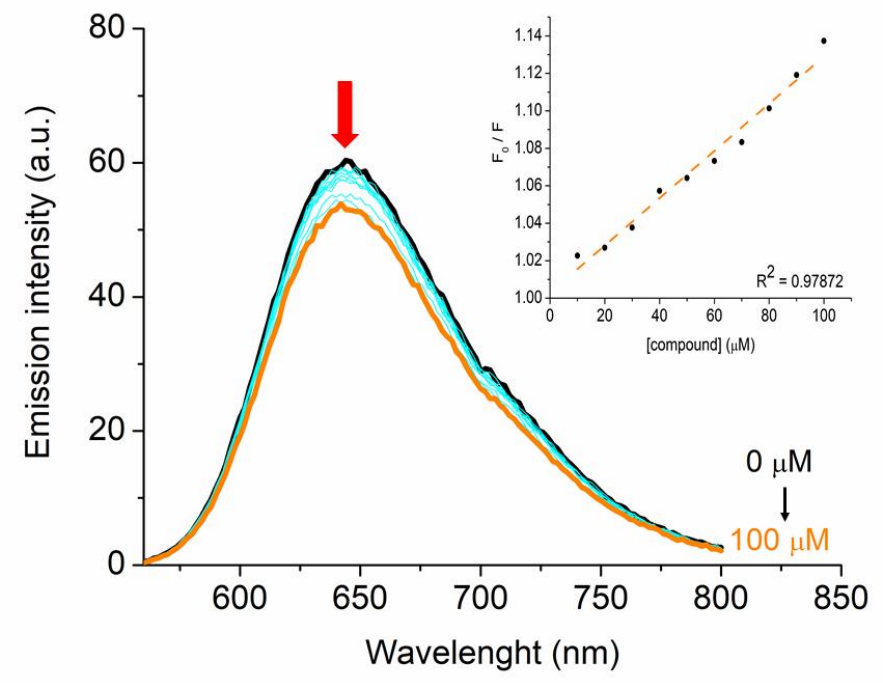

Figure S47. Competitive emission spectra of EB-DNA with derivative **7ac** in a DMSO (2%)/Tris-HCl buffer (pH 7.2) solution. The concentration of compound ranged from 0 to 100 μM. Insert graph shows the plot of F_0/F *versus* [compound].

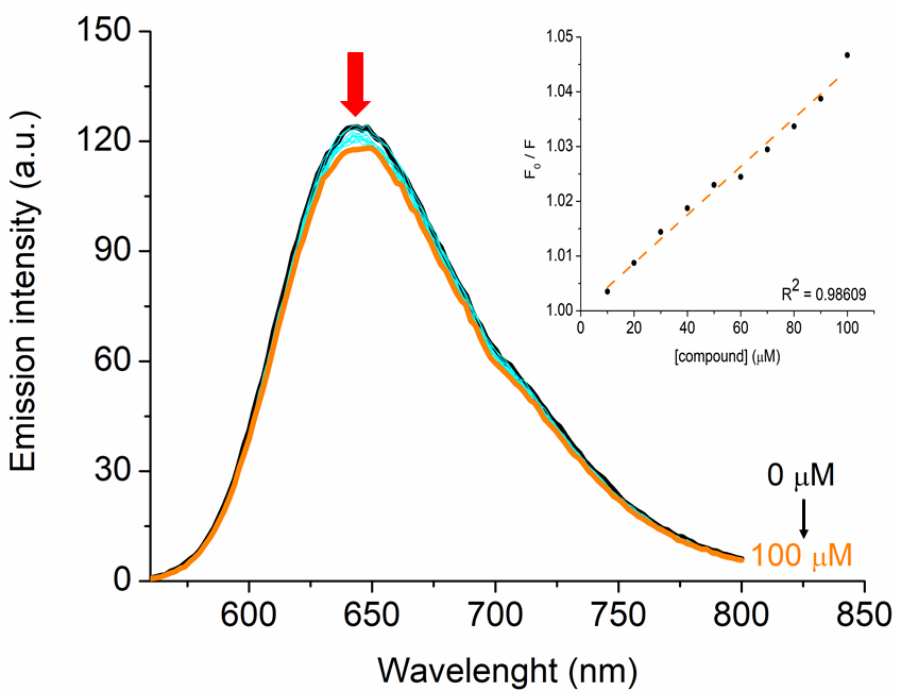

Figure S48. Competitive emission spectra of EB-DNA with derivative **7ad** in a DMSO (2%)/Tris-HCl buffer (pH 7.2) solution. The concentration of compound ranged from 0 to 100 μM. Insert graph shows the plot of F_0/F *versus* [compound].

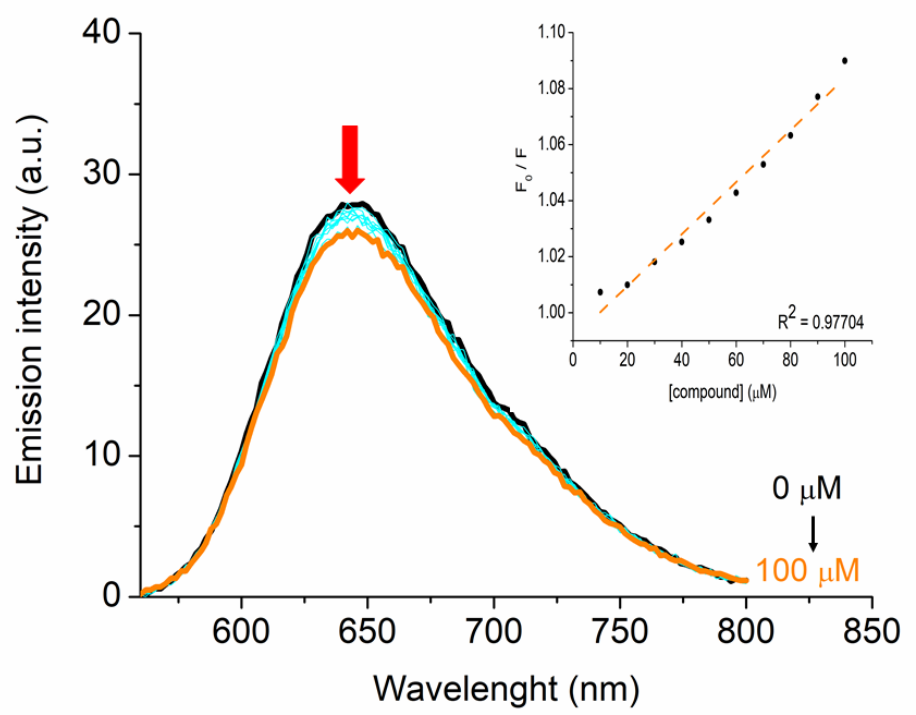

Figure S49. Competitive emission spectra of EB-DNA with derivative **7ae** in a DMSO (2%)/Tris-HCl buffer (pH 7.2) solution. The concentration of compound ranged from 0 to 100 μM. Insert graph shows the plot of F_0/F *versus* [compound].

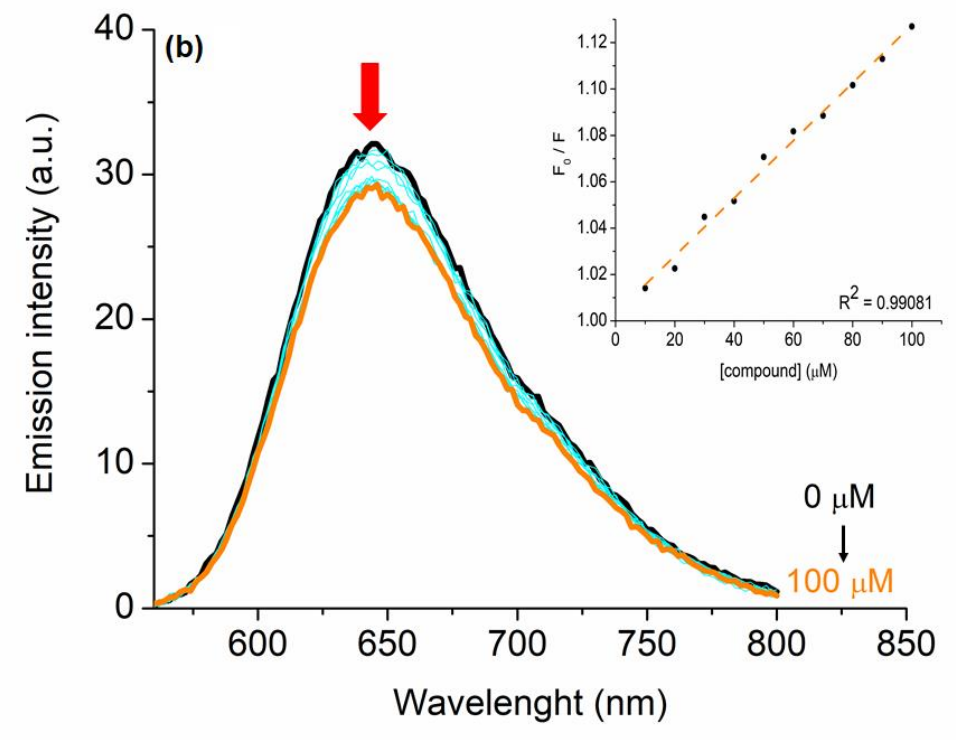

Figure S50. Competitive emission spectra of EB-DNA with derivative **7ba** in a DMSO (2%)/Tris-HCl buffer (pH 7.2) solution. The concentration of compound ranged from 0 to 100 μM. Insert graph shows the plot of F_0/F *versus* [compound].

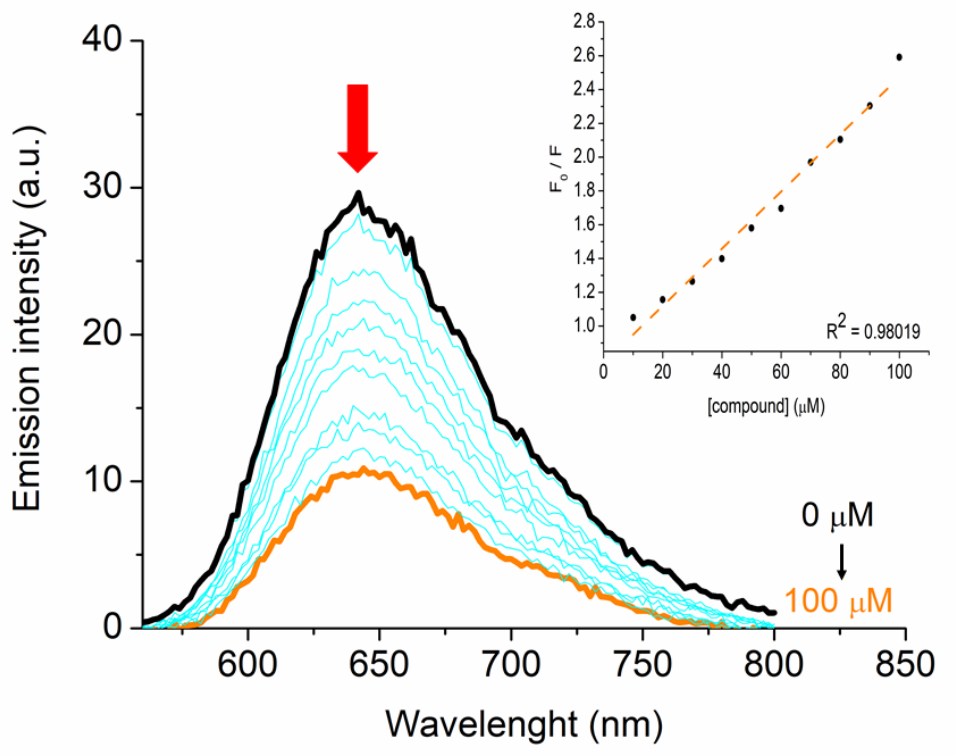

Figure S51. Competitive emission spectra of EB-DNA with derivative **7bb** in a DMSO (2%)/Tris-HCl buffer (pH 7.2) solution. The concentration of compound ranged from 0 to 100 μM. Insert graph shows the plot of F_0/F *versus* [compound].

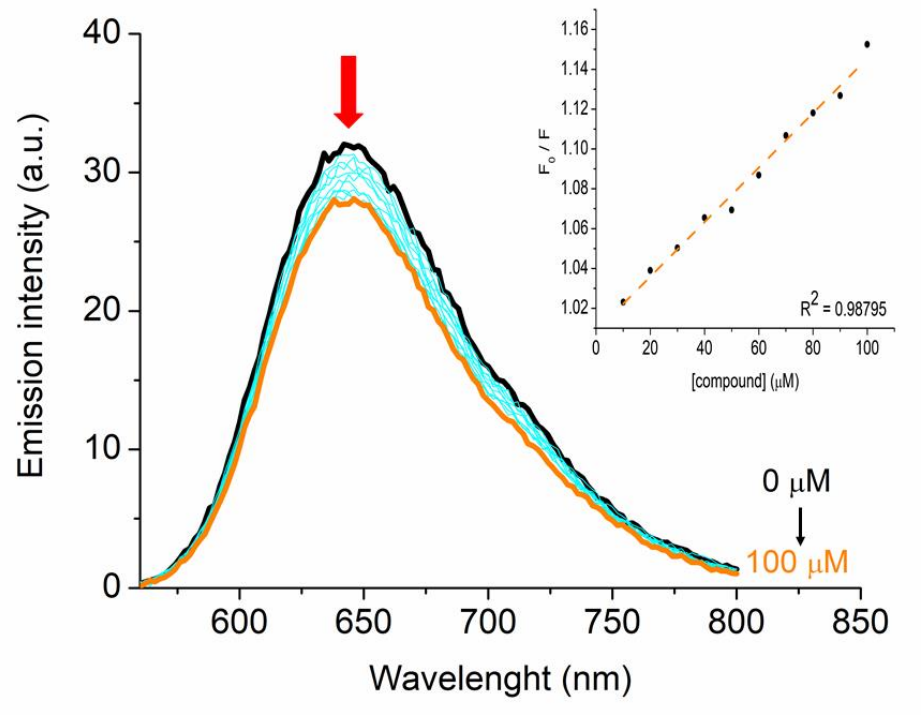

Figure S52. Competitive emission spectra of EB-DNA with derivative **7bc** in a DMSO (2%)/Tris-HCl buffer (pH 7.2) solution. The concentration of compound ranged from 0 to 100 μM. Insert graph shows the plot of F_0/F *versus* [compound].

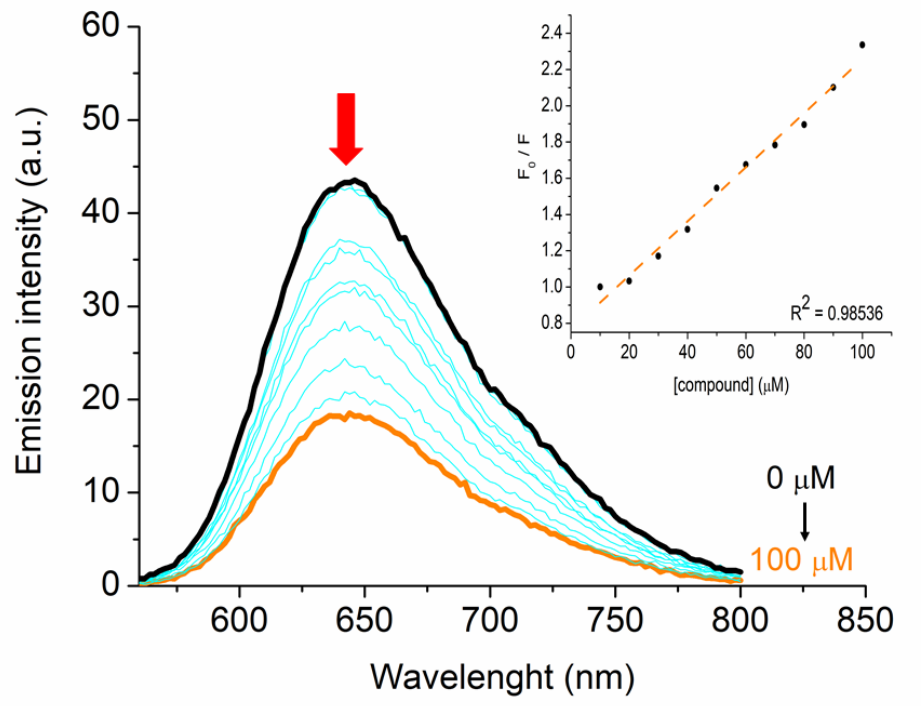

Figure S53. Competitive emission spectra of EB-DNA with derivative **7bd** in a DMSO (2%)/Tris-HCl buffer (pH 7.2) solution. The concentration of compound ranged from 0 to 100 μM. Insert graph shows the plot of F_0/F *versus* [compound].

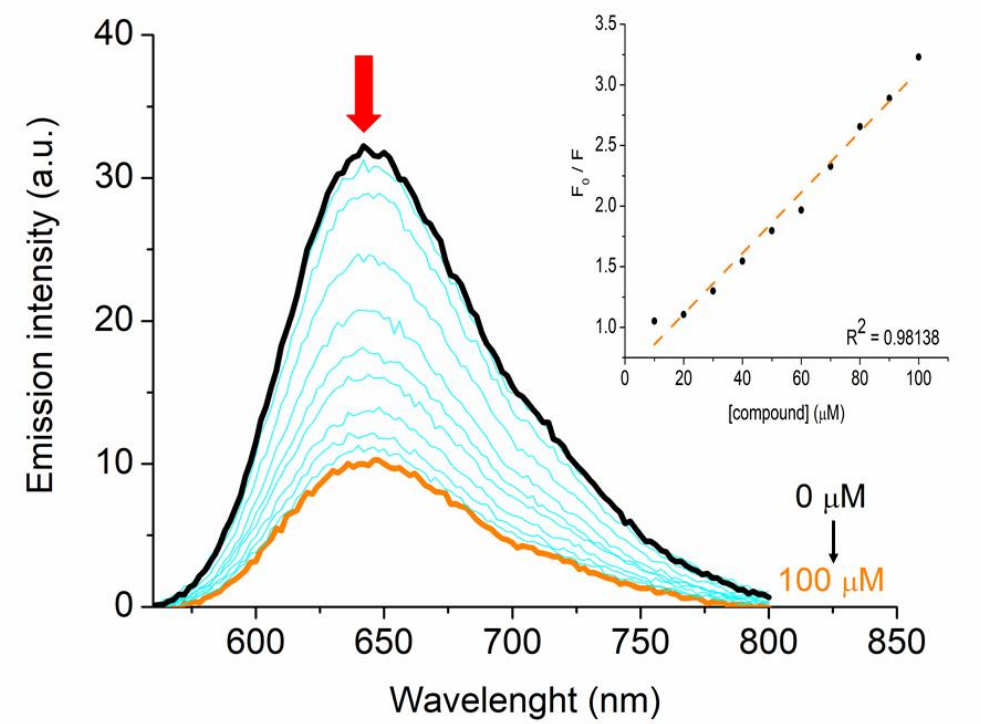

Figure S54. Competitive emission spectra of EB-DNA with derivative **7be** in a DMSO (2%)/Tris-HCl buffer (pH 7.2) solution. The concentration of compound ranged from 0 to 100 μM. Insert graph shows the plot of F_0/F *versus* [compound].

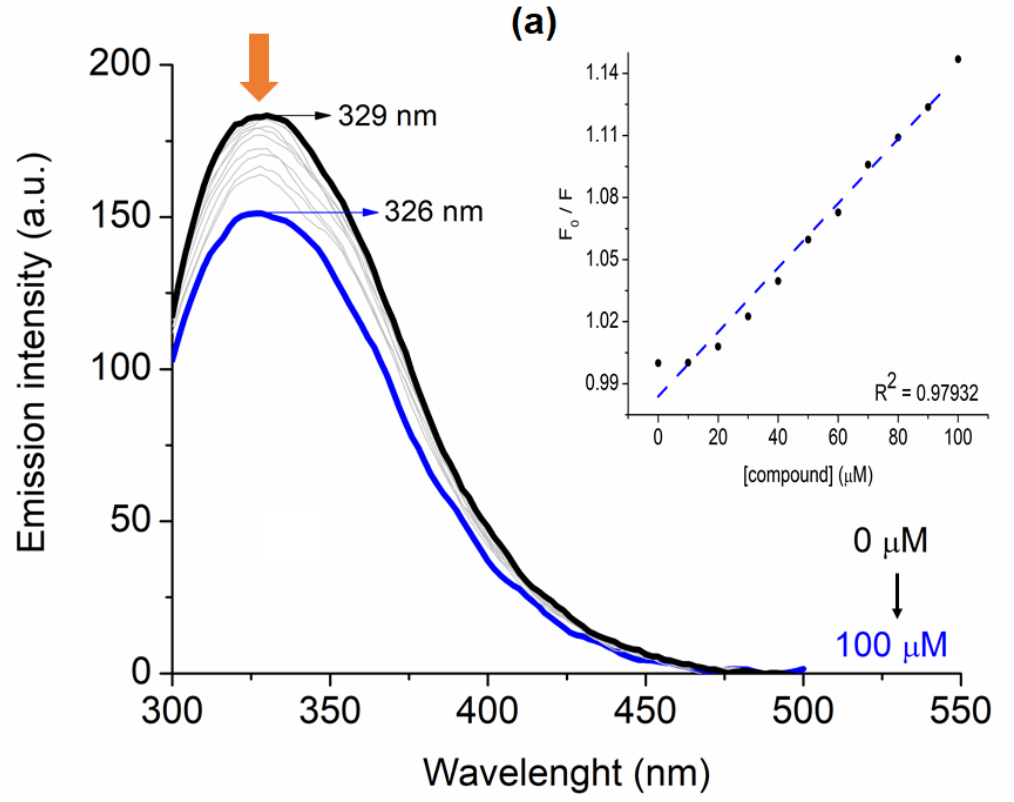

Figure S55. HSA-binding emission spectra with derivative **7aa** in a DMSO (2%)/Tris-HCl buffer (pH 7.2) solution. The concentration of compound ranged from 0 to 100 μM. *Insert graph* shows the plot of F_0/F *versus* [compound].

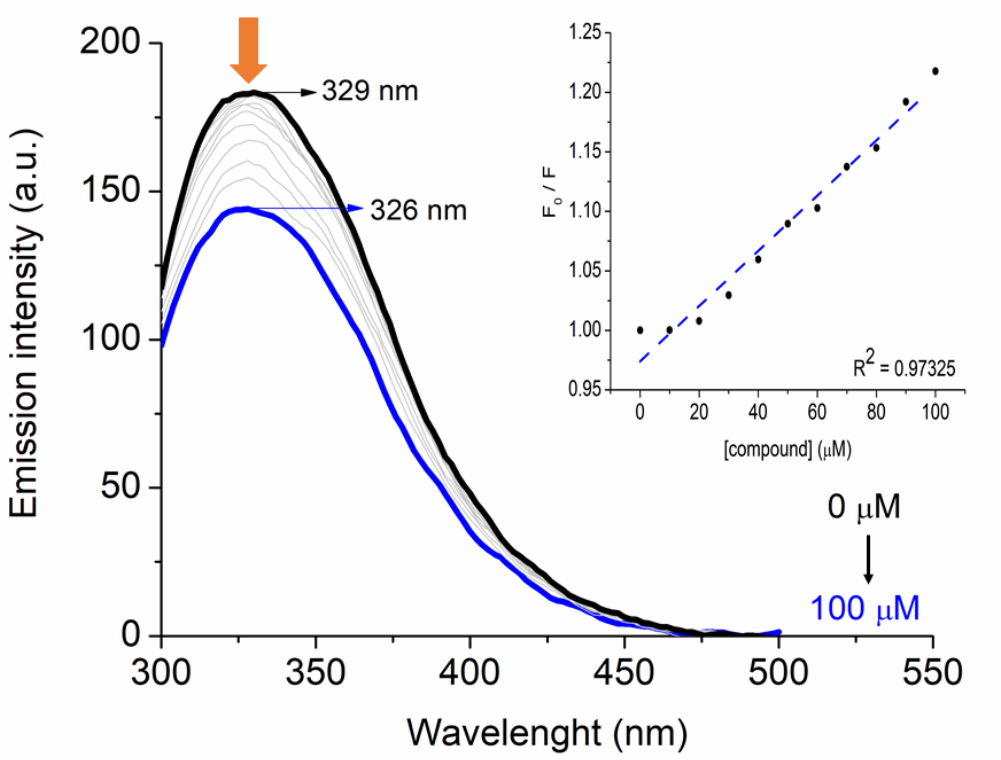

Figure S56. HSA-binding emission spectra with derivative **7ab** in a DMSO (2%)/Tris-HCl buffer (pH 7.2) solution. The concentration of compound ranged from 0 to 100 μM. *Insert graph* shows the plot of F_0/F *versus* [compound].

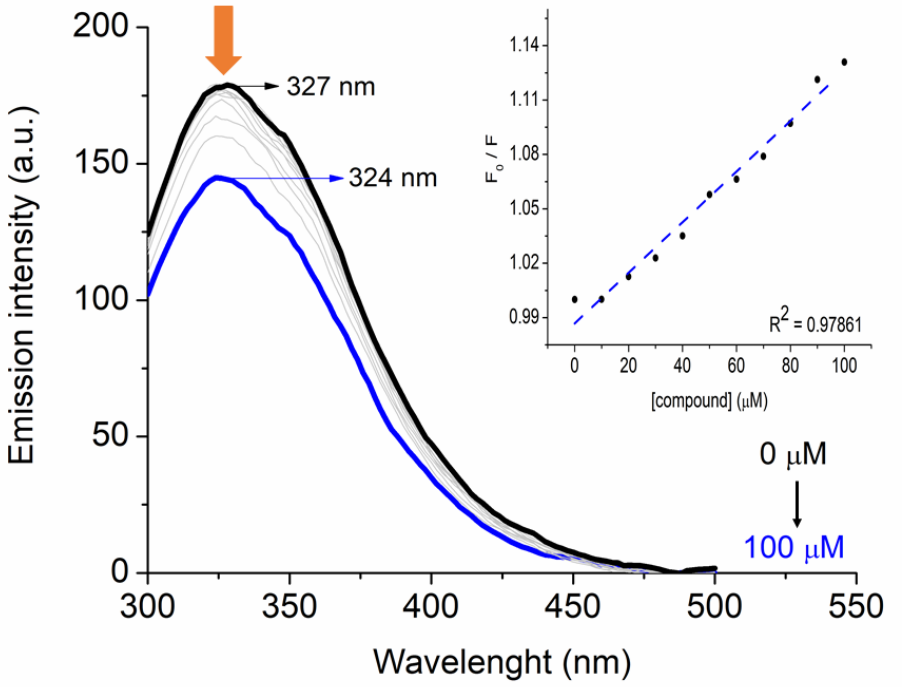

Figure S57. HSA-binding emission spectra with derivative **7ac** in a DMSO (2%)/Tris-HCl buffer (pH 7.2) solution. The concentration of compound ranged from 0 to 100 μM. *Insert graph* shows the plot of F_0/F *versus* [compound].

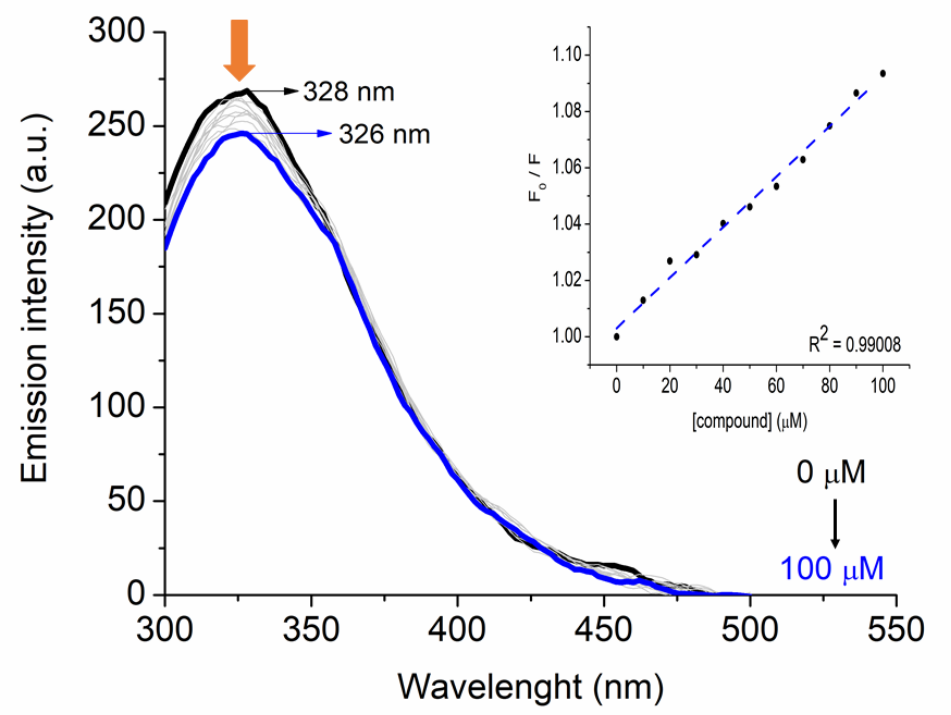

Figure S58. HSA-binding emission spectra with derivative **7ad** in a DMSO (2%)/Tris-HCl buffer (pH 7.2) solution. The concentration of compound ranged from 0 to 100 μM. *Insert graph* shows the plot of F_0/F *versus* [compound].

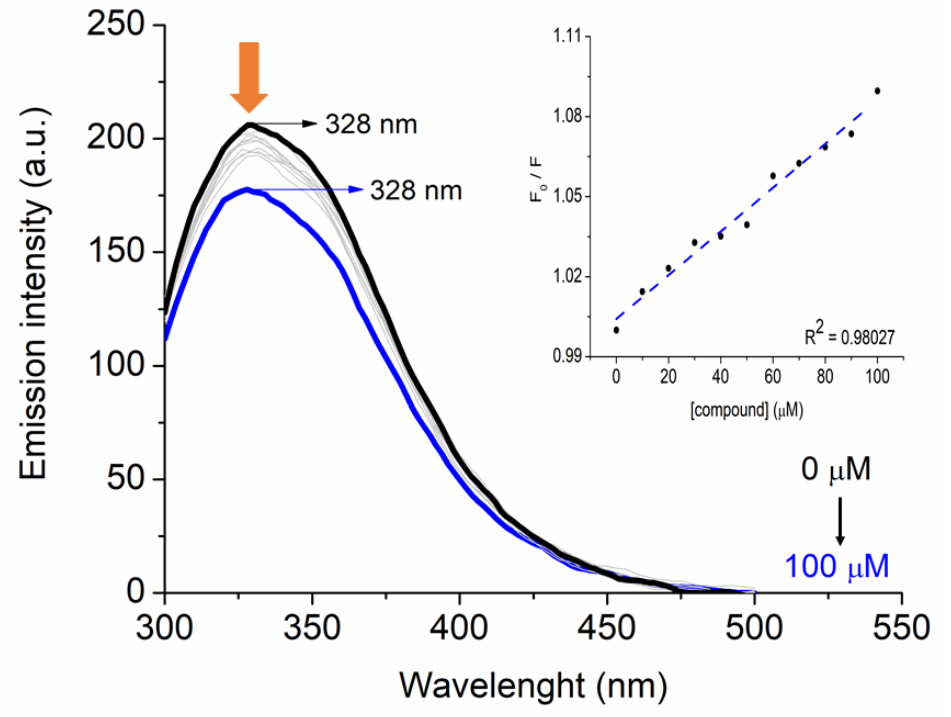

Figure S59. HSA-binding emission spectra with derivative **7ae** in a DMSO (2%)/Tris-HCl buffer (pH 7.2) solution. The concentration of compound ranged from 0 to 100 μM. *Insert graph* shows the plot of F_0/F *versus* [compound].

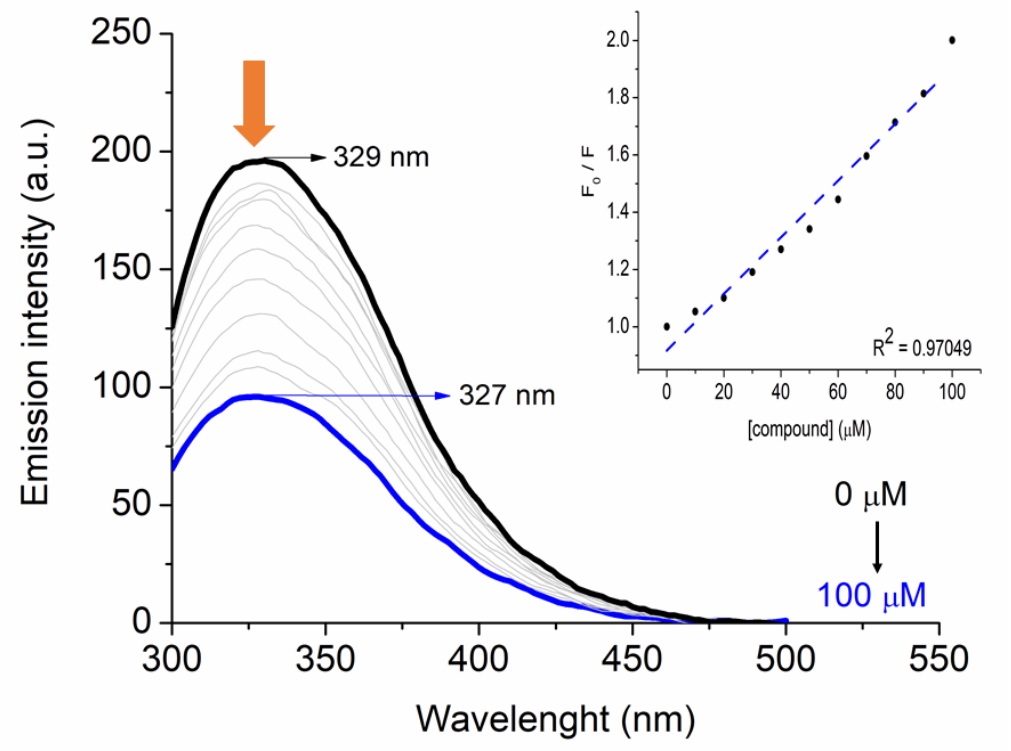

Figure S60. HSA-binding emission spectra with derivative **7bb** in a DMSO (2%)/Tris-HCl buffer (pH 7.2) solution. The concentration of compound ranged from 0 to 100 μM. *Insert graph* shows the plot of F_0/F *versus* [compound].

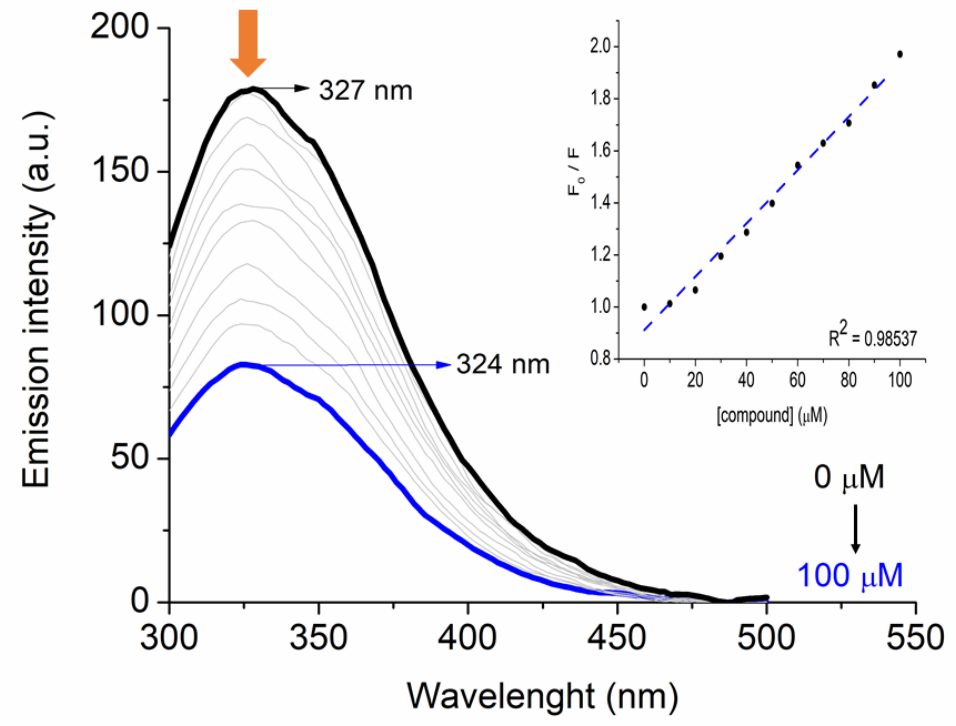

Figure S61. HSA-binding emission spectra with derivative **7bc** in a DMSO (2%)/Tris-HCl buffer (pH 7.2) solution. The concentration of compound ranged from 0 to 100 μM. *Insert graph* shows the plot of F_0/F *versus* [compound].

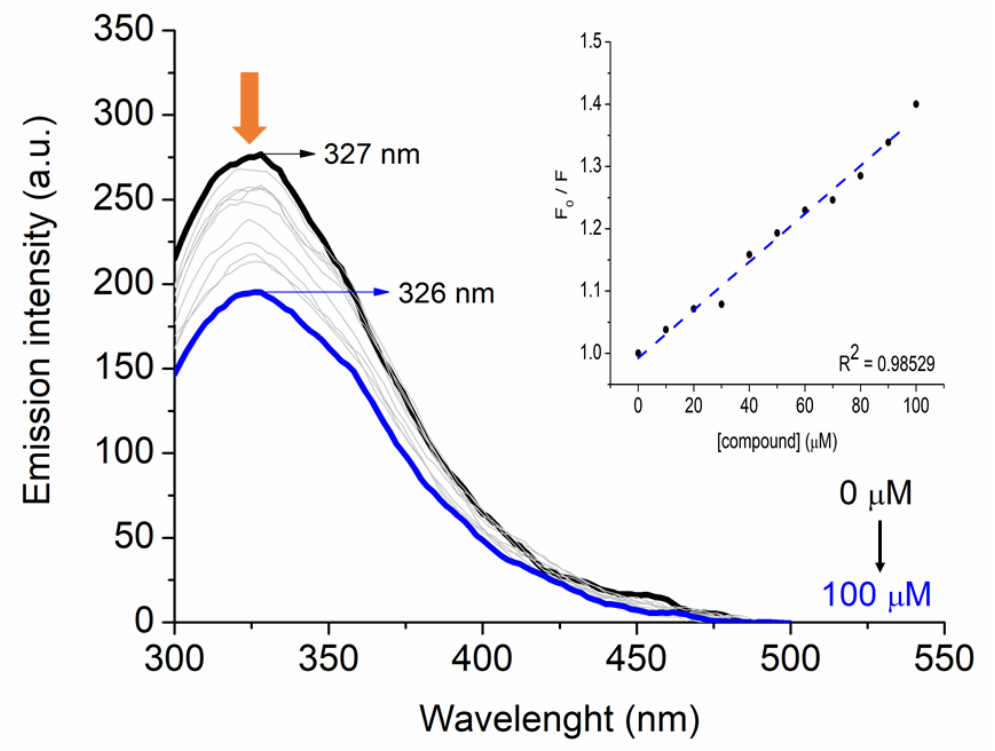

Figure S62. HSA-binding emission spectra with derivative **7bd** in a DMSO (2%)/Tris-HCl buffer (pH 7.2) solution. The concentration of compound ranged from 0 to 100 μM. *Insert graph* shows the plot of F_0/F *versus* [compound].

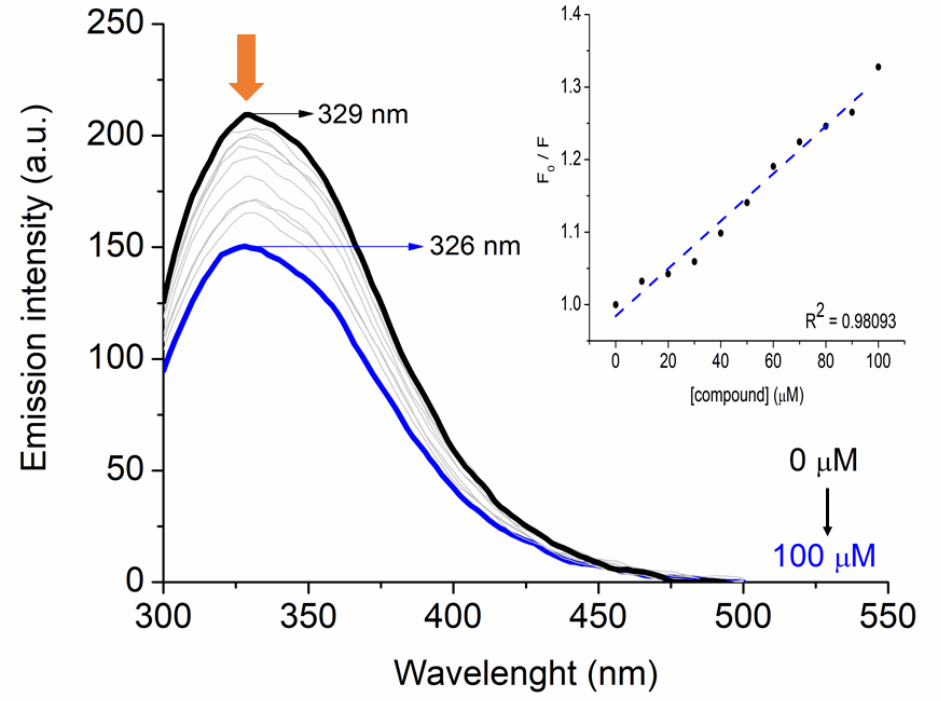

Figure S63. HSA-binding emission spectra with derivative **7be** in a DMSO (2%)/Tris-HCl buffer (pH 7.2) solution. The concentration of compound ranged from 0 to 100 μM. *Insert graph* shows the plot of F_0/F *versus* [compound].

Table S3. The main nucleobases and interactions involved in the association DNA:**7aa-ae** and DNA:**7ba-be** in the minor groove.

Compound	Nucleobase	Interaction	Distance (Å)
7aa-ac, ae	DG-04	Van der Waals	2.30
	DA-05	Van der Waals	2.10
	DA-06	Van der Waals	2.70
	DT-07	Van der Waals	2.40
	DT-08	Van der Waals	2.30
	DA-17	Van der Waals	2.80
	DA-18	Van der Waals	1.70
	DT-19	Van der Waals	2.90
	DT-20	Van der Waals	3.30
	DC-21	Van der Waals	3.40
7ad	DA-06	Van der Waals	2.00
	DT-07	Van der Waals	2.70
	DT-08	Van der Waals	2.40
	DA-18	Van der Waals	2.50
	DT-19	Van der Waals	2.40
	DT-20	Van der Waals	3.00
7ba, bc	DA-05	Van der Waals	3.40
	DA-06	Van der Waals	2.20
	DT-07	Van der Waals	2.40
	DT-08	Van der Waals	2.30
	DC-09	Van der Waals	2.50
	DG-16	Van der Waals	2.80
	DA-17	Van der Waals	2.80
	DA-18	Van der Waals	2.70
	DT-19	Van der Waals	3.00
	DT-20	Van der Waals	2.50
7bb	DA-06	Van der Waals	3.10
	DT-07	Van der Waals	2.60
	DC-09	Van der Waals	2.50
	DG-16	Van der Waals	1.70
	DA-17	Van der Waals	3.00
	DA-18	Van der Waals	3.40
	DT-19	Van der Waals	2.50
7bd, be	DC-03	Van der Waals	3.10
	DG-04	Van der Waals	2.10
	DA-05	Van der Waals	2.60
	DA-06	Van der Waals	1.50
	DT-07	Van der Waals	2.30
	DT-08	Van der Waals	3.00
	DA-18	Van der Waals	2.50
	DT-19	Van der Waals	2.80

	DT-20	Van der Waals	2.90
	DC-21	Van der Waals	3.60
	DG-22	Van der Waals	2.00
	DA-06	Van der Waals	3.60
	DT-07	Van der Waals	2.00
EB	DT-08	Hydrogen bonding	2.90
	DA-17	Van der Waals	3.60
	DA-18	Van der Waals	1.40
	DT-19	Van der Waals	2.40

Table S4. The main amino acid residues and interactions involved in the association HSA:**7aa-ae** and HSA:**7ba-be** in the site II (subdomain IIIA).

Compound	Amino acid residue	Interaction	Distance (Å)
	Ile-388	Van der Waals	1.30
	Tyr-411	Hydrogen bonding	2.10
	Lys-414	Van der Waals	2.80
	Val-415	Van der Waals	2.30
	Val-433	Van der Waals	3.30
7aa-ac	Cys-437	Van der Waals	2.50
	Leu-453	Van der Waals	2.40
	Leu-457	Van der Waals	3.00
	Leu-460	Van der Waals	2.80
	Phe-488	Van der Waals	3.60
	Ser-489	Hydrogen bonding	1.90
	Ile-388	Van der Waals	1.50
	Tyr-411	Hydrogen bonding	2.10
	Leu-430	Van der Waals	2.10
7ad/ae	Val-433	Van der Waals	2.80
	Cys-437	Van der Waals	2.10
	Leu-460	Van der Waals	2.50
	Phe-488	Van der Waals	3.60
	Ser-489	Van der Waals	2.00
	Leu-387	Van der Waals	2.90
	Ile-388	Van der Waals	1.30
	Tyr-411	Hydrogen bonding	2.10
	Val-415	Van der Waals	1.90
7ba-be	Val-418	Van der Waals	1.30
	Val-426	Van der Waals	1.30
	Leu-430	Van der Waals	2.10
	Val-433	Van der Waals	1.70
	Gly-434	Van der Waals	1.90
	Arg-485	Hydrogen bonding	2.70

	Phe-488	Van der Waals	2.30